Universität des Saarlandes

Fachrichtung 6.1 – Mathematik

Preprint

Discrete Transparent Boundary Conditions for the Schrödinger Equation

Anton Arnold and Matthias Ehrhardt

Preprint No. 31

Saarbrücken 2001

Universität des Saarlandes

Fachrichtung 6.1 – Mathematik

Discrete Transparent Boundary Conditions for the Schrödinger Equation

Anton Arnold

Saarland University
Department of Mathematics
Postfach 15 11 50
D–66041 Saarbrücken
Germany
E-Mail: arnold@num.uni-sb.de

Matthias Ehrhardt

Saarland University
Department of Mathematics
Postfach 15 11 50
D–66041 Saarbrücken
Germany
E-Mail: ehrhardt@num.uni-sb.de

submitted: April 2, 2001

Preprint No. 31

Saarbrücken 2001

Edited by
FR 6.1 – Mathematik
Im Stadtwald
D–66041 Saarbrücken
Germany

Fax: + 49 681 302 4443
e-mail: preprint@math.uni-sb.de
WWW: http://www.math.uni-sb.de/

Discrete Transparent Boundary Conditions for the Schrödinger Equation

Abstract

This paper is concerned with transparent boundary conditions for the one dimensional time–dependent Schrödinger equation. They are used to restrict the original PDE problem that is posed on an unbounded domain onto a finite interval in order to make this problem feasible for numerical simulations. The main focus of this article is on the appropriate discretization of such transparent boundary conditions in conjunction with some chosen discretization of the PDE (usually Crank–Nicolson finite differences in the case of the Schrödinger equation). The presented discrete transparent boundary conditions yield an unconditionally stable numerical scheme and are completely reflection–free at the boundary.

1. Introduction

Many physical problems are described mathematically by a partial differential equation (PDE) which is defined on an unbounded domain. If one wants to solve such whole–space evolution problems numerically, one first has to make it finite dimensional. The standard approach is to restrict the computational domain by introducing artificial boundary conditions or absorbing layers. Further possible methods that can be applied are boundary element methods (BEM) (cf. [23]) or infinite element methods (IEM) (see for example [20]). In this paper we focus on the approach of *artificial boundary conditions*.

If the initial data is supported in a finite domain Ω, one can construct boundary conditions (BCs) on $\partial\Omega$ with the objective to approximate the exact solution of the whole–space problem, restricted to Ω. Such BCs are called *absorbing boundary conditions* (ABCs) if they yield a well–posed (initial) boundary value problem (IBVP), where some "energy" is absorbed at the boundary. If the approximate solution coincides on Ω with the exact solution, one refers to these BCs as *transparent boundary conditions* (TBCs). Of course, these boundary conditions should lead to a *well–posed* (initial) boundary value problem. Additionally, it is desirable that the BCs are *local* in space and/or time to allow for an efficient numerical implementation.

In this paper we shall review the state of the art and we shall present recent developments of TBCs for the time-dependent Schrödinger equation. Since quantum mechanical problems are typically posed on a whole space, the "correct" formulation of BCs is of paramount importance for numerical simulations. Due to the wave–like character of the Schrödinger equation the construction and careful discretization of TBCs requires special care. However, most of the ideas presented here carry over to other linear evolution equations like wave or diffusion equations [13].

We remark that Schrödinger–type equations also appear in other fields of application. They arise from *"parabolic" equation* (PE) models which have been widely used for 1–way wave propagation problems in various application areas, e.g. seismology [8], [9], optics and plasma physics (cf. the references in [5]). In underwater acoustics they appear as wide angle approximation to the Helmholtz equation in cylindrical coordinates and are called *wide angle parabolic equations* [24].

The *usual strategy* of employing TBCs for solving a whole–space problem numerically consists of first deriving an *analytic TBC* at the artificial boundary. These TBCs are typically non–local in time (of "memory–type") and can be approximated by a local–in–time BC. Finally, the continuous BC must be discretized to use it with an interior discretization of the PDE. The analytic TBC for the Schrödinger equation was independently derived by several authors from various application fields [3], [6], [21], [30], [33], [35].

While continuous TBCs fully solve the problem of cutting off the spatial domain for the analytical equation, their numerical discretization is far from trivial. Up to now the standard strategy is to derive first the TBC for the analytic equation, then to discretize it, and to use it in connection with some appropriate numerical scheme for the PDE. The defect of this usual approach of discretizing continuous TBCs (*discretized TBCs*) is that the inner discretization of the PDE often does not "match" the discretization of the TBCs. There are two *major problems* of these existing consistent discretizations of the continuous TBC:

P1: The discretized TBCs for the Schrödinger equation often destroy the stability of the whole–space finite difference scheme. E.g. the unconditional stability of the underlying Crank–Nicolson scheme is destroyed [30] and the overall numerical scheme is rendered only *conditionally stable* [6], [30], [34], [42].

P2: The available discretizations often suffer from *reduced accuracy* (in comparison to the discretized whole–space problem) and induce numerical reflections at the boundary, particularly when using coarse grids.

In this paper we discuss in detail a recently developed approach (first outlined in [3]) which overcomes both the *stability problem* (P1) and the problem of *reduced accuracy* (P2). In our *discrete approach* we propose to change the order of the two steps of the usual strategy, i.e. we first consider the discretization of the PDE on the whole space and then derive the TBC for the difference scheme directly on a purely discrete level.

There are several *advantages of the discrete approach.* It completely avoids any numerical reflections at the boundary: no additional discretization errors due to the boundary conditions occur. The discrete TBC is already adapted to the inner scheme and therefore the numerical stability is often better–behaved than for a discretized differential TBC. An additional motivation for this discrete approach arises from the fact that the numerical scheme often needs more boundary conditions than the analytical problem can provide (especially hyperbolic equations, systems of equations and high–order schemes).

In the literature the discrete approach did not gain much attention yet. The first *discrete derivation of artificial boundary conditions* was presented in [15, Section 5]. This discrete approach was also used in [36], [43], [44] for linear hyperbolic systems and in [19] for the wave equation in one dimension, also with error estimates for the reflected part. In [43] a discrete (nonlocal) solution operator for general difference schemes (strictly hyperbolic systems, with constant coefficients in 1D) is constructed. Lill generalized in [26] the approach of Engquist and Majda [15] to boundary conditions for a convection diffusion equation and drops the standard assumption that the initial data is compactly supported inside the computational domain. However, the derived $\mathcal{Z}$–transformed boundary conditions were approximated in order to get local–in–time artificial boundary conditions after the inverse $\mathcal{Z}$–transformation.

Here we construct *discrete transparent boundary conditions* (DTBC) for a Crank–Nicolson finite difference discretization of the Schrödinger equation such that the overall

scheme is unconditionally stable and as accurate as the discretized whole–space problem. The same strategy applies to the θ–scheme for convection diffusion equations [13] and was also used in [12] for the wave equation in the frequency domain.

Although this work concentrates on the discrete derivation of BCs, we will also consider the continuous problem, since the basic ideas of the construction and derivation carry over to the discrete case, e.g. we can use discrete versions of the L^2–estimates. Moreover the well–posedness of the continuous problem is necessary for the stability of the numerical scheme. Just like the analytic TBC, the discrete TBC will be nonlocal in the time variable.

This paper is organized as follows: In Section 2 we first review the continuous TBC for the Schrödinger equation in one space dimension and in §3 we derive and analyze the discrete TBCs which are in the form of a discrete convolution. In order to obtain an efficient implementation one can easily localize these nonlocal in time DTBCs just by cutting off the rapidly decaying sequence of the convolution coefficients. Various numerical examples in Section 3 illustrate the superiority of our DTBC over existing discretizations. In §4 we discuss the DTBC in the case that the initial data is not supported in the computational domain and, finally, in §5 we show how to apply a numerical inverse $\mathcal{Z}$–transform if the exact inverse $\mathcal{Z}$–transform cannot be determined analytically.

2. Transparent Boundary Conditions

In this Section we shall sketch the derivation of the TBC and discuss the well–posedness of the resulting IBVP. Here we will treat the case of the *Schrödinger equation*

$$\begin{aligned} i\hbar\psi_t &= -\frac{\hbar^2}{2}\Delta\psi + V(x,t)\psi, \quad x \in \mathbb{R}, \quad t > 0, \\ \psi(x,0) &= \psi^I(x), \end{aligned} \tag{2.1}$$

where $\psi^I \in L^2(\mathbb{R})$, $V(.,t) \in L^\infty(\mathbb{R})$ and $V(x,.)$ is piecewise continuous.

2.1. Derivation of the TBC. Our goal is to design *transparent boundary conditions (TBCs)* at $x = 0$ and $x = L$, such that the resulting IBVP is well–posed and its solution coincides with the solution of the whole–space problem restricted to $(0, L)$.

We make the following two *basic assumptions*:

A1: The initial data ψ^I is supported in the *computational domain* $0 < x < L$.
A2: The given electrostatic potential is *constant* outside this finite domain: $V(x,t) = 0$ for $x \le 0$, $V(x,t) = V_L$ for $x \ge L$.

Remark 2.1. Without the first assumption information would be lost, and the whole–space evolution could not be reproduced on the finite interval $[0, L]$. The second assumption allows to explicitly solve the equation in the exterior of the computational domain (by the Laplace–method) which is the basic idea of the derivation of the TBC. In Section 4 we will see how to drop the assumption (A1).

We present a formal derivation of the TBC for smooth (i.e. C^1) solutions. Afterwards, the obtained TBC can be regarded for less regular solutions. The first step is to cut the original *whole–space problem* (2.1) into three subproblems, the interior problem on the domain $0 < x < L$, and a left and right exterior problem. They are coupled by the assumption that ψ, ψ_x are continuous across the artificial boundaries at $x = 0$, $x = L$.

The *interior problem* reads

$$
\begin{aligned}
i\hbar\psi_t &= -\frac{\hbar^2}{2}\Delta\psi + V(x,t)\psi, \qquad 0 < x < L, \quad t > 0,\\
\psi(x,0) &= \psi^I(x),\\
\psi_x(0,t) &= (T_0\psi)(0,t),\\
\psi_x(L,t) &= (T_L\psi)(L,t).
\end{aligned}
\tag{2.2}
$$

$T_{0,L}$ denote the *Dirichlet–to–Neumann maps* at the boundaries, and they are obtained by solving the two *exterior problems*:

$$
\begin{aligned}
i\hbar v_t &= -\frac{\hbar^2}{2}\Delta v + V_L v, \qquad x > L, \quad t > 0,\\
v(x,0) &= 0,\\
v(L,t) &= \Phi(t), \qquad t > 0, \qquad \Phi(0) = 0,\\
v(\infty,t) &= 0,\\
(T_L\Phi)(t) &= v_x(L,t),
\end{aligned}
\tag{2.3}
$$

and analogously for T_0. Since the potential is constant in the exterior problems, we can solve them explicitly by the Laplace method and thus obtain the two boundary operators $T_{0,L}$ needed in (2.2). This idea is illustrated in Figure 1.

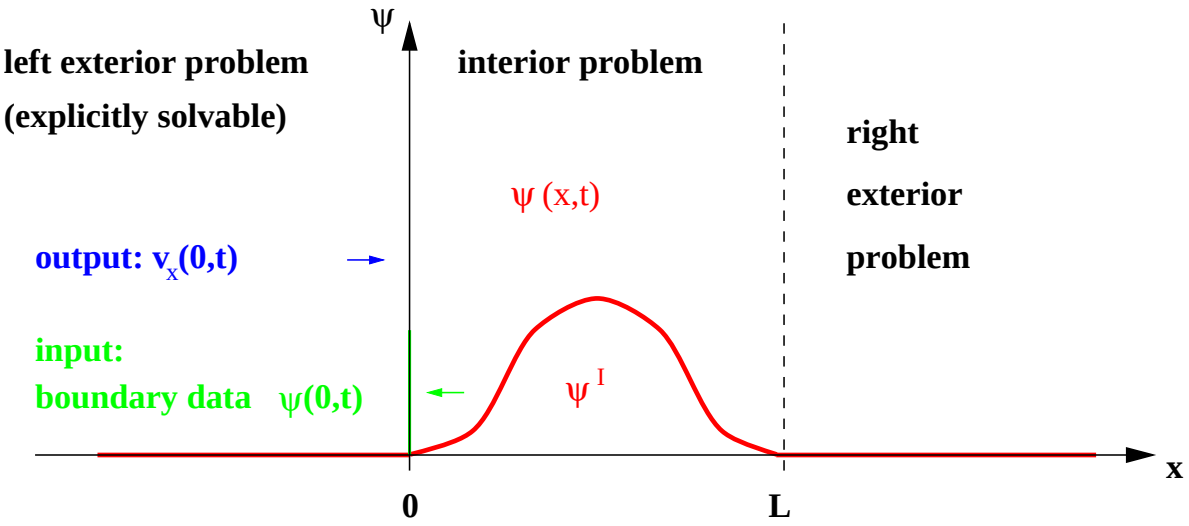

FIGURE 1. Schrödinger equation: Construction idea for transparent boundary conditions

The Laplace transformation of v is given by

$$
\hat{v}(x,s) = \int_0^\infty v(x,t)\, e^{-st}\, dt,
\tag{2.4}
$$

where we set $s = \eta + i\xi$, $\xi \in \mathbb{R}$, and $\eta > 0$ is fixed, with the idea to later perform the limit $\eta \to 0$. Now the right exterior problem (2.3) is transformed to

$$\begin{aligned} &\hat{v}_{xx} + i\frac{2}{\hbar}\big(s + i\frac{V_L}{\hbar}\big)\hat{v} = 0, \quad x > L, \\ &\hat{v}(L,s) = \hat{\Phi}(s). \end{aligned} \tag{2.5}$$

Since its solutions have to decrease as $x \to \infty$ (since we have $\psi(.,t) \in L^2(\mathbb{R})$), we obtain

$$\hat{v}(x,s) = e^{-\sqrt[+]{-i\frac{2}{\hbar}(s+i\frac{V_L}{\hbar})}(x-L)}\hat{\Phi}(s). \tag{2.6}$$

Hence the Laplace–transformed Dirichlet–to–Neumann operator T_L reads

$$\widehat{T_L\Phi}(s) = \hat{v}_x(L,s) = -\sqrt{\frac{2}{\hbar}}\, e^{-i\frac{\pi}{4}} \sqrt[+]{s + i\frac{V_L}{\hbar}}\hat{\Phi}(s), \tag{2.7}$$

and T_0 is calculated analogously. Here, $\sqrt[+]{\ }$ denotes the branch of the square root with nonnegative real part.

An inverse Laplace transformation yields the *right TBC* at $x = L$:

$$\psi_x(L,t) = -\sqrt{\frac{2}{\hbar\pi}}\, e^{-i\frac{\pi}{4}} e^{-i\frac{V_L}{\hbar}t} \frac{d}{dt}\int_0^t \frac{\psi(L,\tau)\, e^{i\frac{V_L}{\hbar}\tau}}{\sqrt{t-\tau}}\, d\tau. \tag{2.8}$$

Similarly, the *left TBC* at $x = 0$ is obtained as

$$\psi_x(0,t) = \sqrt{\frac{2}{\hbar\pi}}\, e^{-i\frac{\pi}{4}} \frac{d}{dt}\int_0^t \frac{\psi(0,\tau)}{\sqrt{t-\tau}}\, d\tau. \tag{2.9}$$

These BCs are *non–local in* t and of memory–type, thus requiring the storage of all previous time levels at the boundary in a numerical discretization. A second difficulty in numerically implementing (2.8), (2.9) is the discretization of the singular convolution kernel. A simple calculation shows that (2.8) is equivalent to the *impedance boundary condition* [33]:

$$\psi(L,t) = -\sqrt{\frac{\hbar}{2\pi}}\, e^{i\frac{\pi}{4}} \int_0^t \frac{\psi_x(L,t-\tau)\, e^{-i\frac{V_L}{\hbar}\tau}}{\sqrt{\tau}}\, d\tau. \tag{2.10}$$

Likewise, (2.9) is equivalent to

$$\psi(0,t) = \sqrt{\frac{\hbar}{2\pi}}\, e^{i\frac{\pi}{4}} \int_0^t \frac{\psi_x(0,\tau)}{\sqrt{t-\tau}}\, d\tau. \tag{2.11}$$

REMARK 2.2 (Inhomogeneous TBC). The (homogeneous) TBC (2.9) was derived for modeling the situation where an initial wave function is supported in the computational domain $[0, L]$, and it is leaving this domain without being reflected back. If an incoming wave function $\psi_{in}(t)$ is given at the left boundary (e.g. a right traveling plane wave), the inhomogeneous TBC

$$\Big[\psi(0,t) - \psi_{in}(0,t)\Big]_x = \sqrt{\frac{2}{\hbar\pi}}\, e^{-i\frac{\pi}{4}} \frac{d}{dt}\int_0^t \frac{\psi(0,\tau) - \psi_{in}(\tau)}{\sqrt{t-\tau}}\, d\tau, \tag{2.12}$$

has to be prescribed at $x = 0$. This is the TBC (2.9) formulated for $\psi(0,t) - \psi_{in}(t)$ since the TBC was only derived for outgoing wave functions. The inhomogeneous TBC is described and analyzed in detail in [4].

REMARK 2.3 (Factorization). It should be noted that the Schrödinger equation can formally be factorized into left and right travelling waves (cf. [6]):

$$\Big(\frac{\partial}{\partial x} - \sqrt{\frac{2}{\hbar}}\, e^{-i\frac{\pi}{4}} \sqrt{\frac{\partial}{\partial t} + i\frac{V_L}{\hbar}}\Big)\Big(\frac{\partial}{\partial x} + \sqrt{\frac{2}{\hbar}}\, e^{-i\frac{\pi}{4}} \sqrt{\frac{\partial}{\partial t} + i\frac{V_L}{\hbar}}\Big)\psi = 0, \tag{2.13}$$

and in the potential–free case:

$$\Big(\frac{\partial}{\partial x} - \sqrt{\frac{2}{\hbar}}\, e^{-i\frac{\pi}{4}} \sqrt{\frac{\partial}{\partial t}}\Big)\Big(\frac{\partial}{\partial x} + \sqrt{\frac{2}{\hbar}}\, e^{-i\frac{\pi}{4}} \sqrt{\frac{\partial}{\partial t}}\Big)\psi = 0, \tag{2.14}$$

where the term

$$\sqrt{\frac{d}{dt}}\,\psi := \frac{1}{\sqrt{\pi}} \frac{d}{dt} \int_0^t \frac{\psi(\tau)}{\sqrt{t-\tau}}\, d\tau \tag{2.15}$$

can be interpreted as a fractional $(\frac{1}{2})$ time derivative.

2.2. Well–posedness of the IBVP. We now turn to the discussion of the well–posedness of (2.2). The existence of a solution to the 1D Schrödinger equation with the TBCs (2.8), (2.9) is clear from the used construction. For regular enough initial data, e.g. $\psi^I \in H^1(0,L)$, the whole–space solution $\psi(x,t)$ will satisfy the TBCs at least in a weak sense. A more detailed discussion is presented in [10].

It remains to check the uniqueness of the solution, i.e. whether the TBC gives rise to spurious solutions. In order to prove uniform boundedness of $\|\psi(.,t)\|_{L^2(0,L)}$ in t we will need the following simple lemma which states that the kernel of the Dirichlet–to–Neumann operator $e^{i\pi/4}\sqrt{d/dt}$ is of *positive type* in the sense of memory equations (see, e.g. [17]).

Using the *Plancherel equality* for the Laplace transformation the following lemma can be shown:

LEMMA 2.4 ([3]). *For any $T > 0$, let $u \in H^{\frac{1}{4}}(0,T)$ with the extension $u(t) = 0$ for $t > T$. Then*

$$\mathrm{Re}\left\{ e^{i\frac{\pi}{4}} \int_0^\infty \bar{u}(t)\, \frac{d}{dt}\Big[\int_0^t \frac{u(s)}{\sqrt{t-s}}\, ds\Big]\, dt \right\} \geq 0. \tag{2.16}$$

With this lemma we shall now derive an estimate for the L^2–norm of solutions to the Schrödinger equation (2.2). We multiply (2.2) by $\bar{\psi}$:

$$\bar{\psi}\psi_t = \frac{i\hbar}{2}\, \bar{\psi}\psi_{xx} - \frac{i}{\hbar}\, V(x,t)\, |\psi|^2, \quad 0 < x < L, \quad t > 0. \tag{2.17}$$

Integrating by parts on $0 < x < L$, and taking the real part gives

$$\begin{aligned} \partial_t \int_0^L |\psi(.,t)|^2\, dx &= \hbar\, \mathrm{Re}\left\{ i\, \bar{\psi}(x,t)\, \psi_x(x,t)\big|_{x=0}^{x=L} \right\} \\ &= -\sqrt{\frac{2\hbar}{\pi}}\, \mathrm{Re}\left\{ e^{i\frac{\pi}{4}}\, \bar{\psi}(L,t)\, e^{-i\frac{V_L}{\hbar}t} \frac{d}{dt} \int_0^t \frac{\psi(L,\tau)\, e^{i\frac{V_L}{\hbar}\tau}}{\sqrt{t-\tau}}\, d\tau \right\} \\ &\quad - \sqrt{\frac{2\hbar}{\pi}}\, \mathrm{Re}\left\{ e^{i\frac{\pi}{4}}\, \bar{\psi}(0,t) \frac{d}{dt} \int_0^t \frac{\psi(0,\tau)}{\sqrt{t-\tau}}\, d\tau \right\}. \end{aligned} \tag{2.18}$$

Now integrating in time and applying Lemma 2.4 for the second term and an analogous lemma for the first term yields the estimate

$$\|\psi(.,t)\|_{L^2(0,L)} \le \|\psi^I\|_{L^2(0,L)}, \quad t > 0. \tag{2.19}$$

This implies uniqueness of the solution to the Schrödinger IBVP. Equation (2.19) reflects the fact that some of the initial mass or particle density $n(x,t) = |\psi(x,t)|^2$ leaves the computational domain $[0,L]$ during the evolution. In the whole–space problem, $x \in \mathbb{R}$, $\|\psi(t)\|_{L^2(\mathbb{R})}$ is of course conserved.

Finally, we address the question of the well–posedness of the Schrödinger equation (2.2) with inhomogeneous TBCs (cf. Remark 2.2). We assume that the incoming wave function $\psi_{in}(t)$ is given at the left boundary by

$$\psi_{in}(x,t) = \alpha\, e^{-i(\omega t + \sqrt{\frac{2}{\hbar}\omega}x)}, \quad \omega \ge 0, \tag{2.20}$$

i.e. a right traveling plane wave. Then the auxiliary function

$$\varphi(x,t) := \psi(x,t) - \Big(1 - \frac{x}{L}\Big)\,\psi_{in}(0,t), \quad 0 \le x \le L, \quad t > 0, \tag{2.21}$$

fulfils the following inhomogeneous Schrödinger equation

$$\begin{aligned} i\hbar\varphi_t &= -\frac{\hbar^2}{2}\Delta\varphi + V(x,t)\varphi + f(x,t), \\ f(x,t) &:= \Big(1 - \frac{x}{L}\Big)\,\psi_{in}(0,t)\big[V(x,t) - \omega\big], \\ \varphi(x,0) &= \varphi^I(x) = \psi^I(x) - \Big(1 - \frac{x}{L}\Big)\,\alpha, \end{aligned} \tag{2.22}$$

with the homogeneous left TBC

$$\Big(\frac{\partial}{\partial x} - \sqrt{\frac{2}{\hbar}}\, e^{-i\frac{\pi}{4}}\sqrt{\frac{\partial}{\partial t}}\Big)\varphi(0,t) = 0, \tag{2.23}$$

and the right TBC (2.8). Proceeding as in the homogeneous case we obtain

$$\partial_t\|\varphi(.,t)\|^2_{L^2(0,L)} \le \frac{1}{\hbar}\,\mathrm{Im}\int_0^L f\bar{\varphi}\,dx \le \frac{1}{\hbar}\|f(.,t)\|_{L^2(0,L)}\|\varphi(.,t)\|_{L^2(0,L)}. \tag{2.24}$$

If we further assume $\|f(.,t)\|_{L^2(0,L)} \le F\hbar$, $t \ge 0$ then it follows easily that

$$\|\psi(.,t)\|_{L^2(0,L)} \le \|\varphi^I\|_{L^2(0,L)} + \alpha\sqrt{\frac{L}{3}} + \frac{F}{2}t, \quad t > 0, \tag{2.25}$$

and this implies the well–posedness.

3. Discrete Transparent Boundary Conditions

In this Section we shall discuss how to discretize the TBC (2.8) in conjunction with a *Crank–Nicolson finite difference scheme* and review the derivation of the DTBC from [3].

With the uniform grid points $x_j = j\Delta x$, $t_n = n\Delta t$, and the approximations $\psi_j^n \sim \psi(x_j,t_n)$ the *discretized Schrödinger equation* (2.1) reads:

$$i\hbar\, D_t^+\psi_j^n = -\frac{\hbar^2}{2}D_x^2\psi_j^{n+\frac{1}{2}} + V_j^{n+\frac{1}{2}}\psi_j^{n+\frac{1}{2}}, \qquad V_j^{n+\frac{1}{2}} = V(x_j,t_{n+\frac{1}{2}}), \tag{3.1}$$

with the time averaging $\psi_j^{n+1/2} = (\psi_j^{n+1} + \psi_j^n)/2$. Here D_t^+ denotes the forward difference quotient in time and D_x^2 is the second order difference quotient in space, i.e.

$$D_t^+ \psi_j^n = \frac{\psi_j^{n+1} - \psi_j^n}{\Delta t}, \quad D_x^2 \psi_j^n = \frac{\psi_{j+1}^n - 2\,\psi_j^n + \psi_{j-1}^n}{(\Delta x)^2}.$$

REMARK 3.1. Most existing discretization schemes for the Schrödinger equation with TBCs are also based on the Crank–Nicolson finite differences ([6], [30], [34]).

For our analysis, one of the main advantages of this *second order* (in Δx and Δt) scheme is, that it is *unconditionally stable* [40] and an easy calculation shows that it preserves the discrete L^2–norm: $\|\psi^n\|_2^2 = \Delta x \sum_{j\in\mathbb{Z}} |\psi_j^n|^2$, which is the discrete analogue of the *mass conservation property* of (2.1).

In order to derive this discrete mass conservation property we multiply (3.1) with $-i\bar{\psi}_j^{n+1/2}/\hbar$:

$$\bar{\psi}_j^{n+\frac{1}{2}} D_t^+ \psi_j^n = \frac{i\hbar}{2}\, \bar{\psi}_j^{n+\frac{1}{2}} D_x^2 \psi_j^{n+\frac{1}{2}} - \frac{i}{\hbar} V_j^{n+\frac{1}{2}} \left|\psi_j^{n+\frac{1}{2}}\right|^2. \tag{3.2}$$

Summing it up for $j \in \mathbb{Z}$ (i.e. in absence of boundary conditions) gives with summation by parts

$$\sum_{j\in\mathbb{Z}} \bar{\psi}_j^{n+\frac{1}{2}} D_t^+ \psi_j^n = -\frac{i\hbar}{2} \sum_{j\in\mathbb{Z}} \left|D_x^+ \psi_j^{n+\frac{1}{2}}\right|^2 - \frac{i}{\hbar} \sum_{j\in\mathbb{Z}} V_j^{n+\frac{1}{2}} \left|\psi_j^{n+\frac{1}{2}}\right|^2. \tag{3.3}$$

Finally, taking the real part by using the simple identity ("*discrete product rule*")

$$D_t^+(\psi^n\, \upsilon^n) = \psi^{n+\frac{1}{2}} D_t^+(\upsilon^n) + \upsilon^{n+\frac{1}{2}} D_t^+(\psi^n), \tag{3.4}$$

i.e. with $\upsilon^n = \bar{\psi}^n$

$$D_t^+ |\psi^n|^2 = 2\,\mathrm{Re}\,\{\bar{\psi}^{n+\frac{1}{2}} D_t^+ \psi^n\}, \tag{3.5}$$

yields the *conservation of the mass* :

$$D_t^+ \sum_{j\in\mathbb{Z}} \left|\psi_j^n\right|^2 = 0. \tag{3.6}$$

REMARK 3.2. We remark that an arbitrary *high (even) order conservative scheme* for the Schrödinger equation (2.1) can be obtained by using the diagonal Padé approximations to the exponential [7]. The Crank–Nicolson scheme corresponds to second order, and the fourth order is known in the ODE literature as *Hammer and Hollingsworth method* [18].

3.1. Discretization strategies for the TBC. We shall now compare three strategies to discretize the TBC (2.8) with its mildly singular convolution kernel. First we review a known discretization from the literature, where the analytic TBC in the equivalent form (2.10) at $L = J\Delta x$ was discretized in an *ad–hoc fashion.*

Discretized TBC of Mayfield. In [30] Mayfield proposed the approximation

$$\begin{aligned}\int_0^{t_n} \frac{\psi_x(L, t_n - \tau)\, e^{-i\frac{V_L}{\hbar}\tau}}{\sqrt{\tau}}\, d\tau &\approx \frac{1}{\Delta x} \sum_{m=0}^{n-1} (\psi_J^{n-m} - \psi_{J-1}^{n-m})\, e^{-i\frac{V_L}{\hbar} m\Delta t} \int_{t_m}^{t_{m+1}} \frac{d\tau}{\sqrt{\tau}} \\ &= \frac{2\sqrt{\Delta t}}{\Delta x} \sum_{m=0}^{n-1} \frac{(\psi_J^{n-m} - \psi_{J-1}^{n-m})\, e^{-i\frac{V_L}{\hbar} m\Delta t}}{\sqrt{m+1} + \sqrt{m}},\end{aligned} \tag{3.7}$$

where she used the left–point rectangular quadrature rule. This leads to the following *discretized TBC* for the Schrödinger equation:

$$\psi_J^n - \psi_{J-1}^n = \frac{\Delta x}{2B\sqrt{\Delta t}}\,\psi_J^n - \sum_{m=1}^{n-1}\left(\psi_J^{n-m} - \psi_{J-1}^{n-m}\right)\tilde{\ell}_m, \tag{3.8}$$

with

$$B = -\sqrt{\frac{\hbar}{2\pi}}\,e^{i\frac{\pi}{4}}, \qquad \tilde{\ell}_m = \frac{e^{-i\frac{V_L}{\hbar}m\Delta t}}{\sqrt{m+1}+\sqrt{m}}.$$

On the fully discrete level this BC is no longer perfectly transparent. For the resulting scheme with a homogeneous Dirichlet BC at $j = 0$ and (3.8), Mayfield obtained the following result:

THEOREM 3.3 ([30]). *The numerical scheme* (3.1), (3.8) *is stable, if and only if*

$$4\pi\hbar\,\frac{\Delta t}{\Delta x^2} \in \bigcup_{j\in\mathbb{N}_0}\left[(2j+1)^{-2},(2j)^{-2}\right]. \tag{3.9}$$

This shows that the chosen discretization of the TBC (3.8) destroys the unconditional stability of the underlying Crank–Nicolson scheme. The *stability regions* of Theorem 3.3 are illustrated in Figure 2 as light areas. The dark intervals are regions of instability.

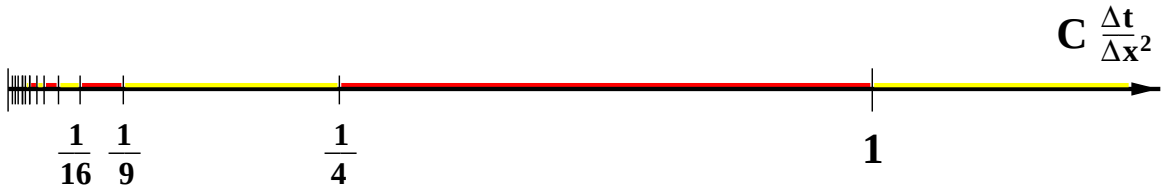

FIGURE 2. Discretized TBC of Mayfield: Stability regions.

As the numerical example in Section 3.5 will show this discretization gives rise to unphysical reflections at the boundary.

REMARK 3.4 (Approach of Baskakov and Popov). A similar strategy using a higher-order quadrature rule for the l.h.s. of (3.7) was introduced by Baskakov and Popov in [6]. This approach typically induces less numerical reflections compared to the results when using the discretized TBC of Mayfield.

Semi–Discrete TBC of Schmidt and Deuflhard. In the *semi–discrete approach* of Schmidt and Deuflhard [38] a TBC is derived for the semi–discretized (in t) Schrödinger equation. This method also applies for a nonuniform in t (e.g. adaptive) interior scheme and it admits a time–dependent potential in the exterior domain (i.e. $V_L = V_L(t)$). While being *unconditionally stable* (in conjunction with an interior finite element scheme) [39], it still exhibits small residual reflections at the artificial boundary. In [39] this approach is also applied to uniform exterior z–discretizations, and one then recovers — through a different derivation — the discrete TBC from [3].

Approach of Lubich and Schädle. The time discretization is done by the trapezoidal rule in the interior and by convolution quadrature on the boundary. The numerical integration of the convolution integral is done in the following way (cf. [27], [28] [37]). If $\hat{f}(s)$ denotes the Laplace transform of f, then formally setting $s = \partial_t$ yields

$$\begin{aligned} \hat{f}(\partial_t)\, g(t) &= \int_0^\infty f(\tau)\, e^{-\tau \partial_t} g(t)\, d\tau \\ &= \int_0^\infty f(\tau)\, g(t-\tau)\, d\tau \\ &= f * g, \end{aligned} \tag{3.10}$$

where g is a function satisfying $g(t) = 0$ for $t < 0$. Now $\hat{f}(\partial_t)\, g(t)$ is approximated by the *discrete convolution*

$$\hat{f}(\partial_t)\, g(t) := \sum_{n \geq 0} \omega_n\, g(t - nk), \tag{3.11}$$

with the stepsize $k = \Delta t$. The quadrature weights ω_n are defined as the coefficients of the generating power series:

$$\sum_{n \geq 0} \omega_n\, \xi^n := \hat{f}\left(\frac{\delta(\xi)}{k}\right), \quad |\xi| \text{ small}. \tag{3.12}$$

Here $\delta(\xi) = \sum_{n=0}^{\infty} \delta_n \xi^n$ is the quotient of the generating polynomials of a linear multistep method, e.g. $\delta(\xi) = 2(1-\xi)/(1+\xi)$ for the trapezoidal rule. If one chooses for the quadrature the same numerical scheme as in the interior then one obtains also a reflection–free discrete TBC.

Discrete TBC. Instead of using an ad–hoc discretization of the analytic TBC like (3.7) we will construct *discrete TBCs* of the fully discretized whole–space problem. Our new strategy solves both problems of the *discretized TBC* at no additional computational costs. With our DTBC the numerical solution on the computational domain $0 \leq j \leq J$ exactly equals the discrete whole–space solution (on $j \in \mathbb{Z}$) restricted to the computational domain. Therefore, our overall scheme prevents any numerical reflections at the boundary and inherits the unconditional stability of the whole–space Crank–Nicolson scheme (see Theorem 3.13). These different approaches, discretization of the analytic TBC and (semi–)discrete TBC, are sketched in Figure 3.

Consequently, when considering the discretization of TBCs, it should be a standard strategy to derive the *discrete TBCs* of the fully discretized problem, rather then attempting to discretize the differential TBC whenever it is possible. A comparison of these two strategies for a 1D wave propagation problem is given in [12].

3.2. Derivation of the DTBC. To derive the discrete TBC we will now mimick the derivation of the analytic TBC from Section 2 on a discrete level. The Crank–Nicolson scheme (3.1) can be written in the form:

$$-iR\,(\psi_j^{n+1} - \psi_j^n) = \Delta_x^2 \psi_j^{n+1} + \Delta_x^2 \psi_j^n + w V_j^{n+\frac{1}{2}} (\psi_j^{n+1} + \psi_j^n), \tag{3.13}$$

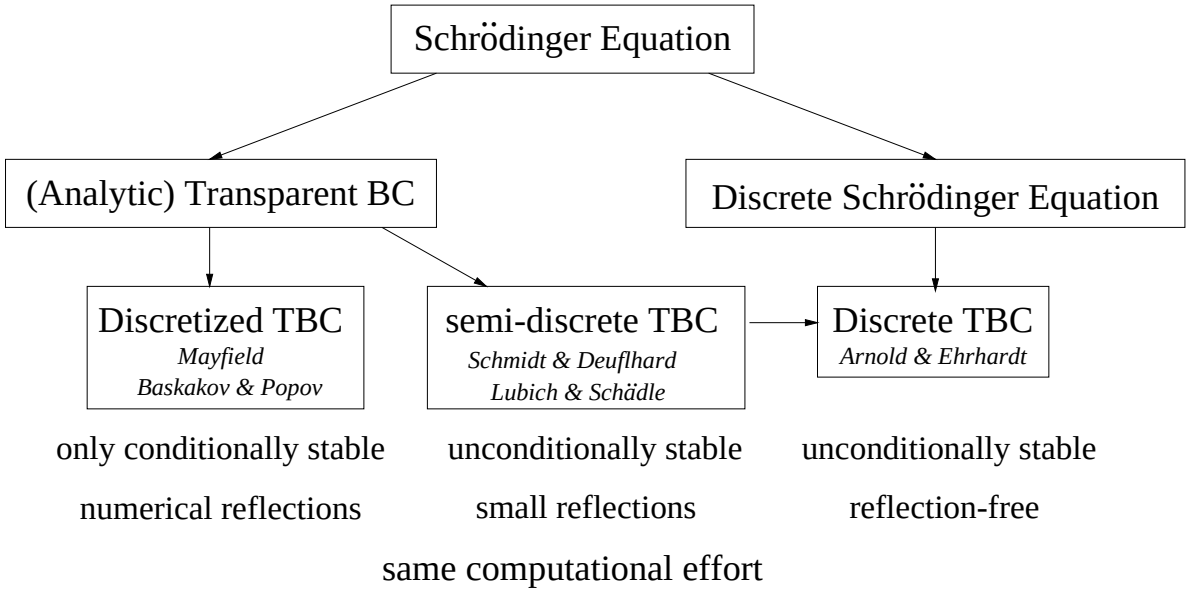

FIGURE 3. Discretization strategies for the TBC

with

$$R = \frac{4}{\hbar}\frac{(\Delta x)^2}{\Delta t}, \quad w = -\frac{2(\Delta x)^2}{\hbar^2}, \quad V_j^{n+\frac{1}{2}} = V(x_j, t_{n+\frac{1}{2}}),$$

where $\Delta_x^2 \psi_j^n = \psi_{j+1}^n - 2\,\psi_j^n + \psi_{j-1}^n$, and R is proportional to the parabolic mesh ratio.

Again, we will only consider the right BC. In analogy to the continuous problem we assume for the potential and initial data: $V_j^n = V_L = \text{const}$, $j \geq J-1$, $\psi_j^0 = 0$, $j \geq J-2$ and solve the discrete right exterior problem by using the discrete analogue of the Laplace transformation, the *$\mathcal{Z}$–transform*:

$$\mathcal{Z}\{\psi_j^n\} = \hat{\psi}_j(z) := \sum_{n=0}^{\infty} \psi_j^n\, z^{-n}, \quad z \in \mathbb{C}, \quad |z| > 1. \tag{3.14}$$

Hence, the $\mathcal{Z}$–transformed Crank–Nicolson finite difference scheme (3.13) for $j \geq J-1$ reads

$$(z+1)\Delta_x^2 \hat{\psi}_j(z) = -iR\big[z - 1 + i\kappa(z+1)\big]\hat{\psi}_j(z), \quad \kappa = \frac{\Delta t}{2}\frac{V_L}{\hbar}. \tag{3.15}$$

The two linearly independent solutions of the resulting *second order difference equation*

$$\hat{\psi}_{j+1}(z) - 2\left[1 - \frac{iR}{2}\Big(\frac{z-1}{z+1} + i\kappa\Big)\right]\hat{\psi}_j(z) + \hat{\psi}_{j-1}(z) = 0, \qquad j \geq J-1, \tag{3.16}$$

take the form $\hat{\psi}_j(z) = \nu_{1,2}^j(z)$, $j \geq J-1$, where $\nu_{1,2}(z)$ solve

$$\nu^2 - 2\left[1 - \frac{iR}{2}\Big(\frac{z-1}{z+1} + i\kappa\Big)\right]\nu + 1 = 0. \tag{3.17}$$

For the decreasing mode (as $j \to \infty$) we have to require $|\nu_1(z)| < 1$ and obtain (using $\nu_1(z)\nu_2(z) = 1$) the *$\mathcal{Z}$–transformed right DTBC* as

$$\hat{\psi}_{J-1}(z) = \nu_2(z)\,\hat{\psi}_J(z). \tag{3.18}$$

Analogously, the *$\mathcal{Z}$–transformed left DTBC* reads:

$$\hat{\psi}_1(z) = \tilde{\nu}_2(z)\,\hat{\psi}_0(z), \tag{3.19}$$

where $\tilde{\nu}_2(z)$ with $|\tilde{\nu}_2(z)| > 1$ is obtained from a solution to the *left discrete problem*, i.e. (3.16) on the range $j \leq 1$.

REMARK 3.5 (Discrete Factorization). If S denotes the usual *shift operator* given by $S\hat{\psi}_j(z) = \hat{\psi}_{j+1}(z)$, then analogously to the continuous case (cf. Remark 2.3) the discretized Schrödinger equation (3.16) can formally be factorized as:

$$\big(S - \nu_1(z)\big)\big(S - \nu_2(z)\big)\,\hat{\psi}_j(z) = 0, \qquad j \geq J-1, \tag{3.20}$$

which leads to the same DTBCs (3.18), (3.19).

It remains to inverse transform (3.18) using the inversion rules of the $\mathcal{Z}$-transform (cf. [11], e.g.). By the following tedious calculation this can be achieved explicitly.

CALCULATION (of $\mathcal{Z}^{-1}\{\nu_2(z)\}$). First we rewrite $\nu_{1,2}(z)$ as:

$$\begin{aligned}\nu_{1,2}(z) &= 1 - \frac{iR}{2}\Big(\frac{z-1}{z+1} + i\kappa\Big) \pm \sqrt[+]{-\frac{iR}{2}\Big(\frac{z-1}{z+1} + i\kappa\Big)\Big[2 - \frac{iR}{2}\Big(\frac{z-1}{z+1} + i\kappa\Big)\Big]} \\ &= 1 + \frac{iR}{2} + \frac{R\kappa}{2} - iR\frac{z}{z+1} \mp \frac{iR}{2}\frac{1}{z+1}\sqrt[+]{Az^2 - 2Bz + C},\end{aligned} \tag{3.21}$$

with the constants

$$A = (1+i\kappa)\Big(1 + i\kappa + i\frac{4}{R}\Big), \tag{3.22a}$$

$$B = 1 + \kappa^2 + \frac{4\kappa}{R}, \tag{3.22b}$$

$$C = (1-i\kappa)\Big(1 - i\kappa - i\frac{4}{R}\Big). \tag{3.22c}$$

For the inverse $\mathcal{Z}$–transform we use

$$\sqrt[+]{Az^2 - 2Bz + C} = \frac{1}{\sqrt[+]{A}}\,\frac{Az^2 - 2Bz + C}{z}\,\frac{\frac{\sqrt[+]{A}}{\sqrt[+]{C}}\,z}{\sqrt[+]{\frac{A}{C}z^2 - 2\frac{B}{C}z + 1}}. \tag{3.23}$$

With the abbreviations

$$F(z,\mu) = \frac{z}{\sqrt[+]{z^2 - 2\mu z + 1}}, \quad \lambda = \frac{\sqrt[+]{A}}{\sqrt[+]{C}}, \quad \mu = \frac{B}{\sqrt[+]{A}\,\sqrt[+]{C}}, \tag{3.24}$$

we obtain from equation (3.23)

$$\begin{aligned}\frac{1}{z+1}\sqrt[+]{Az^2 - 2Bz + C} &= \frac{1}{\sqrt[+]{A}}\,\frac{Az^2 - 2Bz + C}{z(z+1)}\,F(\lambda z,\mu) \\ &= \frac{1}{\sqrt[+]{A}}\left\{A + \frac{C}{z} - \frac{E}{z+1}\right\}F(\lambda z,\mu) \\ &= \sqrt[+]{C}\left\{\lambda + \lambda^{-1}\frac{1}{z} - \frac{E}{\sqrt[+]{A}\,\sqrt[+]{C}}\frac{1}{z+1}\right\}F(\lambda z,\mu),\end{aligned} \tag{3.25}$$

with $E = A + 2B + C$. The inversion rules now yield

$$\begin{aligned}\mathcal{Z}^{-1}\left\{\frac{\sqrt[+]{Az^2-2Bz+C}}{z+1}\right\} &= \sqrt[+]{C}\left\{\lambda\delta_n^0+\lambda^{-1}\delta_n^1-\frac{E}{\sqrt[+]{A}\,\sqrt[+]{C}}\left[(-1)^n-\delta_n^0\right]\right\}*\widetilde{P}_n(\mu)\\ &= \sqrt[+]{C}\left\{\lambda\widetilde{P}_n(\mu)+\lambda^{-1}\widetilde{P}_{n-1}(\mu)-\frac{E}{\sqrt[+]{A}\,\sqrt[+]{C}}\sum_{k=0}^{n-1}(-1)^{n-k}\widetilde{P}_k(\mu)\right\},\end{aligned}$$

where $*$ denotes the discrete convolution. Finally, we obtain

(3.26)
$$\begin{aligned}\mathcal{Z}^{-1}\left\{\nu_{1,2}(z)\right\} &= \left[1-i\frac{R}{2}+\frac{R\kappa}{2}\right]\delta_n^0+iR(-1)^n\\ &\quad\mp\frac{iR\sqrt[+]{C}}{2}\lambda^{-n}\left\{\lambda P_n(\mu)+P_{n-1}(\mu)-\frac{E}{\sqrt[+]{A}\,\sqrt[+]{C}}\sum_{k=0}^{n-1}(-\lambda)^{n-k}P_k(\mu)\right\}.\end{aligned}$$

Since $C = \bar{A}$ we have $|\lambda| = 1$ with

$$\lambda = \frac{A}{\sqrt[+]{A}\,\sqrt[+]{C}} = \frac{R-4\kappa-R\kappa^2+2i(R\kappa+2)}{\sqrt{(1+\kappa^2)\left[R^2+(R\kappa+4)^2\right]}}. \tag{3.27}$$

Therefore we write

$$\lambda = e^{i\varphi}, \quad \text{with} \quad \varphi = \arg\frac{2(R\kappa+2)}{R-4\kappa-R\kappa^2}. \tag{3.28}$$

We obtain for the parameter μ:

$$\mu = \frac{R(1+\kappa^2)+4\kappa}{\sqrt{(1+\kappa^2)\left[R^2+(R\kappa+4)^2\right]}} \in \mathbb{R}, \tag{3.29}$$

and it can easily be seen that $-1 < \mu < 1$ is valid. The constant E simply equals 4 and we get

$$\tau = \frac{E}{\sqrt[+]{A}\,\sqrt[+]{C}} = \frac{4R}{\sqrt{(1+\kappa^2)\left[R^2+(R\kappa+4)^2\right]}} \in \mathbb{R}. \tag{3.30}$$

The choice of the sign in (3.26) can be justified analytically or simply by testing it numerically. We finally obtain the *convolution coefficients* $\ell^{(n)} = \mathcal{Z}^{-1}\left\{\nu_2(z)\right\}$ as

$$\begin{aligned}\ell^{(n)} &= \left[1+i\frac{R}{2}+\frac{\sigma}{2}\right]\delta_n^0-iR(-1)^n-\frac{i}{2}\sqrt[4]{(R^2+\sigma^2)\left[R^2+(\sigma+4)^2\right]}\,e^{-i\varphi/2}\cdot\\ &\quad\cdot e^{-in\varphi}\left\{\lambda P_n(\mu)+P_{n-1}(\mu)-\tau\sum_{k=0}^{n-1}(-\lambda)^{n-k}P_k(\mu)\right\},\end{aligned} \tag{3.31}$$

with $\sigma = R\kappa$ and P_n denotes the Legendre polynomials. The resulting *discrete TBCs* at the grid points x_j, $j = 0, J$ read

$$\psi_1^n - \ell_0^{(0)}\psi_0^n = \sum_{k=1}^{n-1} \ell_0^{(n-k)}\psi_0^k, \quad n \geq 1, \tag{3.32a}$$

$$\psi_{J-1}^n - \ell_J^{(0)}\psi_J^n = \sum_{k=1}^{n-1} \ell_J^{(n-k)}\psi_J^k, \quad n \geq 1. \tag{3.32b}$$

The subscript j of the coefficients $\ell^{(n)}$ indicates at which boundary the values are to be taken. In the sequel many parameters will be supplied with this subscript.

3.3. The Asymptotic Behaviour of the Convolution Coefficients. We study the asymptotic behaviour of the $\ell_0^{(n)}$, $\ell_J^{(n)}$ in (3.32). It will turn out that it is advantageous to reformulate the DTBC using new coefficients. Afterwards we shall derive a recursion formula for these new coefficients and compare their decay rate with the decay rate of the continuous integral kernel in (2.8), (2.9).

The summed convolution coeffcients. First we want to study the *asymptotic behaviour* of the convolution coefficients $\ell_j^{(n)}$, $j = 0, J$. With the notation $\mu_j = \cos\theta_j$, $0 < \theta_j < \pi$, we use the following classical result on the *asymptotic property of the Legendre polynomials*:

LEMMA 3.6 (Theorem 8.21.2 (Formula of Laplace), [41]).

$$P_n(\cos\theta_j) = \frac{\sqrt{2}}{\sqrt{\pi}\sqrt{\sin\theta_j}} \frac{\cos\left[(n+\frac{1}{2})\theta_j - \frac{\pi}{4}\right]}{\sqrt{n}} + \mathrm{O}(n^{-3/2}), \quad 0 < \theta_j < \pi. \tag{3.33}$$

The bound for the error term holds uniformly in the interval $\varepsilon \leq \theta_j \leq \pi - \varepsilon$.

From this lemma we conclude that $\lim_{n\to\infty} P_n(\mu_j) = 0$ holds. Consequently, the coefficients have the following asymptotic behaviour for $n \to \infty$:

$$\ell_j^{(n)} - iR(-1)^n \sim \frac{i\tau_j}{2}\sqrt[4]{(R^2+\sigma_j^2)\left[R^2+(\sigma_j+4)^2\right]}\, e^{-i\varphi_j/2}(-1)^n \sum_{k=0}^{n-1}(-e^{-i\varphi_j})^k P_k(\mu_j). \tag{3.34}$$

Using

$$\begin{aligned}\lim_{n\to\infty}\sum_{k=0}^{n-1}(-e^{-i\varphi_j})^k P_k(\mu_j) &= \frac{1}{\sqrt{1+2\mu_j\bar{\lambda}_j+\bar{\lambda}_j{}^2}} = \frac{1}{\sqrt{2\lambda_j}}\frac{1}{\sqrt{\mathrm{Re}\ \lambda_j+\mu_j}} \\ &= \frac{1}{2R}\sqrt[4]{(R^2+\sigma_j^2)\left[R^2+(\sigma_j+4)^2\right]}\, e^{i\varphi_j/2},\end{aligned} \tag{3.35}$$

we finally obtain

$$\ell_j^{(n)} \sim iR(-1)^n + \frac{i\tau_j}{4R}\sqrt{(R^2+\sigma_j^2)\left[R^2+(\sigma_j+4)^2\right]}(-1)^n = 2iR(-1)^n. \tag{3.36}$$

The sequence $\ell_j^{(n)}$ is asymptotically an alternating, purely imaginary sequence, which may lead (on the numerical level) to subtractive cancellation in (3.32). To circumvent

this problem we consider the *summed coefficients*

$$s_j^{(n)} := \ell_j^{(n)} + \ell_j^{(n-1)}, \quad n \geq 1, \quad s_j^{(0)} := \ell_j^{(0)}, \quad j = 0, J, \tag{3.37}$$

and compute:

$$\begin{aligned} \ell_j^{(0)} &= 1 - i\frac{R}{2} + \frac{\sigma_j}{2} - \frac{i}{2}\sqrt[4]{(R^2+\sigma_j^2)\left[R^2+(\sigma_j+4)^2\right]}\, e^{i\varphi_j/2} \\ &= 1 - i\frac{R}{2} + \frac{\sigma_j}{2} - \frac{i}{2}\sqrt[+]{R^2 - 4\sigma_j - \sigma_j^2 + 2iR(\sigma_j+2)}, \end{aligned} \tag{3.38}$$

$$\ell_j^{(1)} = iR - \frac{i}{2}\sqrt[4]{(R^2+\sigma_j^2)\left[R^2+(\sigma_j+4)^2\right]}\, e^{-i\varphi_j/2}\left\{\mu_j + e^{-i\varphi_j} + \tau_j\right\}, \tag{3.39}$$

and for $n \geq 2$ we compute using the definition of E:

$$\begin{aligned} s_j^{(n)} = &-\frac{i}{2}\sqrt[4]{(R^2+\sigma_j^2)\left[R^2+(\sigma_j+4)^2\right]}\, e^{i\varphi_j/2}\, e^{-in\varphi_j} \\ &\Big\{P_n(\mu_j) + \underbrace{\left(\lambda_j + \lambda_j^{-1} - \tau_j\right)}_{=-2\mu_j} P_{n-1}(\mu_j) + P_{n-2}(\mu_j)\Big\}. \end{aligned} \tag{3.40}$$

With the recurrence relation of the Legendre polynomials

$$\mu_j P_{n-1}(\mu_j) = \frac{n}{2n-1}P_n(\mu_j) + \frac{n-1}{2n-1}P_{n-2}(\mu_j), \quad n \geq 1,$$

we finally get

$$s_j^{(n)} = \frac{i}{2}\sqrt[4]{(R^2+\sigma_j^2)\left[R^2+(\sigma_j+4)^2\right]}\, e^{i\varphi_j/2}\, e^{-in\varphi_j}\, \frac{P_n(\mu_j) - P_{n-2}(\mu_j)}{2n-1}, \quad n \geq 2. \tag{3.41}$$

REMARK 3.7. The coefficient $\ell_j^{(0)}$ can also be calculated with [11, Theorem 39.1] by

$$\ell_j^{(0)} = \lim_{z\to\infty} \nu_2(z) = 1 - i\frac{R}{2} + \frac{\sigma_j}{2} - \frac{i}{2}\sqrt[+]{(R+i\sigma_j)(R+i(\sigma_j+4))}. \tag{3.42}$$

We summarize our results in the following theorem:

THEOREM 3.8 ([3]). *The left (at $j = 0$) and right (at $j = J$) discrete TBCs for the Crank–Nicolson discretization* (3.1) *of the 1D Schrödinger equation are respectively*

$$\psi_1^n - s_0^{(0)}\psi_0^n = \sum_{k=1}^{n-1} s_0^{(n-k)}\psi_0^k - \psi_1^{n-1}, \quad n \geq 1, \tag{3.43a}$$

$$\psi_{J-1}^n - s_J^{(0)}\psi_J^n = \sum_{k=1}^{n-1} s_J^{(n-k)}\psi_J^k - \psi_{J-1}^{n-1}, \quad n \geq 1, \tag{3.43b}$$

with

$$s_j^{(n)} = \left[1 - i\frac{R}{2} + \frac{\sigma_j}{2}\right]\delta_n^0 + \left[1 + i\frac{R}{2} + \frac{\sigma_j}{2}\right]\delta_n^1 + \alpha_j\, e^{-in\varphi_j}\, \frac{P_n(\mu_j) - P_{n-2}(\mu_j)}{2n-1}, \tag{3.44}$$

$$\varphi_j = \arctan\frac{2R(\sigma_j+2)}{R^2 - 4\sigma_j - \sigma_j^2}, \quad \mu_j = \frac{R^2 + 4\sigma_j + \sigma_j^2}{\sqrt{(R^2+\sigma_j^2)\left[R^2+(\sigma_j+4)^2\right]}},$$

$$\sigma_j = \frac{2\Delta x^2}{\hbar^2}V_j, \quad \alpha_j = \frac{i}{2}\sqrt[4]{(R^2+\sigma_j^2)\left[R^2+(\sigma_j+4)^2\right]}\, e^{i\varphi_j/2}, \quad j = 0, J.$$

P_n denotes the Legendre polynomials ($P_{-1} \equiv P_{-2} \equiv 0$) and δ_n^j the Kronecker symbol.

The P_n only have to be evaluated at the two values $\mu_0, \mu_J \in (-1, 1)$, and hence the numerically stable recursion formula for the Legendre polynomials can be used [16].

The recurrence formula for the summed coefficients. In this subsection we shall give two different derivations for the recursion formula of the convolution coefficients $s_j^{(n)}$. The first one is based on the explicit representation (3.41) of $s_j^{(n)}$ by first calculating a recursion formula for $P_{n+1}(\mu_j) - P_{n-1}(\mu_j)$. The second derivation does not require the explicit form of the coefficients $s_j^{(n)}$ but only the *growth functions* $\nu_{1,2}(z)$ from the $\mathcal{Z}$–transformed DTBCs (3.18) and (3.19).

First Derivation: Here we start with the *standard recursion formula* [1] for the Legendre polynomials $P_{n+1}(\mu_j)$, $P_{n-1}(\mu_j)$:

$$\begin{aligned}(n+1)P_{n+1}(\mu_j) &= (2n+1)\mu_j P_n(\mu_j) - nP_{n-1}(\mu_j), \qquad n \geq 0,\\ (n-1)P_{n-1}(\mu_j) &= (2n-3)\mu_j P_{n-2}(\mu_j) - (n-2)P_{n-3}(\mu_j), \qquad n \geq 2,\end{aligned} \tag{3.45}$$

and

$$P_{n-1}(\mu_j) - 2\mu_j P_{n-2}(\mu_j) + P_{n-3}(\mu_j) = \frac{P_{n-3}(\mu_j) - P_{n-1}(\mu_j)}{2n-3}, \qquad n \geq 2. \tag{3.46}$$

The expression $P_{n+1}(\mu_j) - P_{n-1}(\mu_j)$ is converted in the following way:

$$\begin{aligned}&(n+1)\big[P_{n+1}(\mu_j) - P_{n-1}(\mu_j)\big]\\ &\quad= (2n+1)\mu_j P_n(\mu_j) - (2n+1)\frac{2n-3}{n-1}\mu_j P_{n-2}(\mu_j) + (2n+1)\frac{n-2}{n-1}P_{n-3}(\mu_j)\\ &\quad= (2n+1)\mu_j\big[P_n(\mu_j) - P_{n-2}(\mu_j)\big] - \frac{(n-2)(2n+1)}{2n-3}\big[P_{n-1}(\mu_j) - P_{n-3}(\mu_j)\big],\end{aligned}$$

where we have used the relation

$$\begin{aligned}P_{n-3}(\mu_j) - \mu_j P_{n-2}(\mu_j) &= \frac{1}{2}\left[\frac{P_{n-3}(\mu_j) - P_{n-1}(\mu_j)}{2n-3} - P_{n-1}(\mu_j) + P_{n-3}(\mu_j)\right]\\ &= -\frac{n-1}{2n-3}\big[P_{n-1}(\mu_j) - P_{n-3}(\mu_j)\big].\end{aligned}$$

Finally, we obtain for $n \geq 2$ the following recursion formula for $P_{n+1}(\mu_j) - P_{n-1}(\mu_j)$:

$$\begin{aligned}&P_{n+1}(\mu_j) - P_{n-1}(\mu_j) =\\ &\qquad\frac{2n+1}{n+1}\mu_j\big[P_n(\mu_j) - P_{n-2}(\mu_j)\big] - \frac{(n-2)(2n+1)}{(n+1)(2n-3)}\big[P_{n-1}(\mu_j) - P_{n-3}(\mu_j)\big].\end{aligned} \tag{3.47}$$

Since the $s_j^{(n)}$ are determined by

$$s_j^{(n)} = \alpha_j \frac{\lambda_j^{-n}}{2n-1}\big[P_n(\mu_j) - P_{n-2}(\mu_j)\big], \quad n \geq 2, \tag{3.48}$$

we get from (3.47) the *recurrence relation* for the summed convolution coefficients:

$$s_j^{(n+1)} = \frac{2n-1}{n+1}\mu_j\lambda_j^{-1}s_j^{(n)} - \frac{n-2}{n+1}\lambda_j^{-2}s_j^{(n-1)}, \quad n \geq 2, \tag{3.49}$$

which can be used after calculating the first values $s_j^{(n)}$ for $n = 0, 1, 2$ by the formula (3.44).

SECOND DERIVATION: Next we shall present an alternative derivation of the first convolution coefficients $s_j^{(n)}$, $n = 0, 1, 2$ and the recurrence relation (3.49). The advantage of this alternative approach is that we shall only need the *growth functions* $\nu_{1,2}(z)$ from the $\mathcal{Z}$–transformed DTBCs (3.18) and (3.19). Hence this approach might also apply to a bigger class of linear evolution equations, where it is not possible (or too tedious) to derive an explicit representation of the convolution coefficients.

We remark that an even more advantageous approach might be based on the polynomial equation (3.17) for the growth function $\nu(z)$, rather than on its explicit solution. The benefit of such a strategy would lie in the possibility to obtain the convolution coefficients also for higher order difference schemes, that would lead to quartic (or even higher order) equations for $\nu(z)$. To our knowledge this has, however, not been accomplished yet.

In this second approach we shall first derive a first order ODE for the growth function $\nu(z)$, which is explicitly given by (3.21). In fact, it is more convenient to consider

$$\tilde{\nu}(z) := (z+1)\nu(z) = \sum_{n=-1}^{\infty} s_j^{(n+1)} z^{-n}. \tag{3.50}$$

Using the constants (3.22) and (3.24) it has the explicit form

(3.51)

$$\tilde{\nu}_{1,2}(z) = z\Big(1 - \frac{iR}{2} + \frac{\sigma_j}{2}\Big) + \Big(1 + \frac{iR}{2} + \frac{\sigma_j}{2}\Big) \pm \frac{i}{2}\sqrt{R^2 + 4\sigma_j + \sigma_j^2}\,\sqrt{z^2\frac{\lambda}{\mu} - 2z + \frac{1}{\lambda\mu}}\,.$$

The index $j = 0, J$ again denotes the grid point where the DTBC is to be constructed. Multiplying $\tilde{\nu}' = \dfrac{d\tilde{\nu}}{dz}$ by $\Big(z^2\dfrac{\lambda}{\mu} - 2z + \dfrac{1}{\lambda\mu}\Big)$ then yields an inhomogeneous first order ODE for $\tilde{\nu}(z)$:

$$\Big(z^2\frac{\lambda}{\mu} - 2z + \frac{1}{\lambda\mu}\Big)\,\tilde{\nu}(z)' - \Big(z\frac{\lambda}{\mu} - 1\Big)\,\tilde{\nu}(z) = \beta(z) := \beta_{-1}z + \beta_0, \tag{3.52}$$

with

$$\begin{aligned} \beta_{-1} &= -\frac{\lambda}{\mu}\Big(1 + \frac{iR}{2} + \frac{\sigma_j}{2}\Big) + \Big(-1 + \frac{iR}{2} - \frac{\sigma_j}{2}\Big), \\ \beta_0 &= \frac{1}{\lambda\mu}\Big(1 - \frac{iR}{2} + \frac{\sigma_j}{2}\Big) + \Big(1 + \frac{iR}{2} + \frac{\sigma_j}{2}\Big). \end{aligned} \tag{3.53}$$

Its general solution includes $\tilde{\nu}_{1,2}(z)$ as defined in (3.51). Using the Laurent series (3.50) of $\tilde{\nu}$ and $\tilde{\nu}'$ in (3.52) immediately yields the desired recursion for the coefficients $s_j^{(n)}$:

$$\begin{aligned} -\frac{\lambda}{\mu}s_j^{(1)} - s_j^{(0)} &= \beta_{-1}, \\ -2\frac{\lambda}{\mu}s_j^{(2)} + s_j^{(1)} + \frac{1}{\lambda\mu}s_j^{(0)} &= \beta_0, \\ -(n+1)s_j^{(n+1)} + (2n-1)\frac{\mu}{\lambda}s_j^{(n)} - (n-2)\frac{1}{\lambda^2}s_j^{(n-1)} &= 0, \quad n \geq 2, \end{aligned} \tag{3.54}$$

which coincides with (3.49).

The starting coefficient of the recursion can be determined as in (3.42):

$$s_j^{(0)} = \lim_{z\to\infty} \frac{\tilde{\nu}(z)}{z} = 1 - i\frac{R}{2} + \frac{\sigma_j}{2} \pm \frac{i}{2}\sqrt{R^2 + 4\sigma_j + \sigma_j^2}\,\sqrt{\frac{\lambda}{\mu}}.$$

Here, the sign has to be fixed such that $|\nu_1(z)| < 1$ for the right DTBC and $|\nu_2(z)| > 1$ for the left DTBC. This can be done for e.g. for $z = \infty$.

Stability of the Recurrence Relation: For proving that the recurrence relation (3.49) is *well–conditioned* we follow the notation in [16] and write (3.49) as the second order difference equation

$$s_j^{(n+1)} + a_j^{(n)} s_j^{(n)} + b_j^{(n)} s_j^{(n-1)} = 0, \quad n \geq 2, \tag{3.55}$$

with

$$a_j^{(n)} = -\frac{2n-1}{n+1}\,\mu_j\lambda_j^{-1}, \qquad b_j^{(n)} = \frac{n-2}{n+1}\,\lambda_j^{-2} \neq 0. \tag{3.56}$$

There are two linearly independent solutions $s_{j,1}^{(n)}$, $s_{j,2}^{(n)}$ to (3.55). If they have the property

$$\lim_{n\to\infty} \frac{s_{j,2}^{(n)}}{s_{j,1}^{(n)}} = 0 \tag{3.57}$$

then $s_{j,2}^{(n)}$ is called a *minimal solution* and serious numerical problems arise if one tries to compute the solution $s_{j,2}^{(n)}$ in *a* straightforward way by using the recursion (3.49): A (small) initial error would induce arbitrarily large relative errors in $s_{j,2}^{(n)}$, even when evaluating the recursion (3.49) with infinite precision. Methods of calculating minimal solutions of three–term recurrence relations can be found in [16]. To prove that (3.49) is well–conditioned we have to show that the seeked solution is not a minimal solution to (3.55). This type of solution is called *dominant*.

Since the coefficients $a_j^{(n)}$, $b_j^{(n)}$ in (3.55) have the finite limits

$$a_j = \lim_{n\to\infty} a_j^{(n)} = -2\mu_j\lambda_j^{-1} = -2\frac{B_j}{A_j}, \qquad b_j = \lim_{n\to\infty} b_j^{(n)} = \lambda_j^{-2} = \frac{C_j}{A_j}, \quad j = 0, J, \tag{3.58}$$

one calls (3.55) a *Poincaré difference equation* and

$$\Phi_j(t) = t^2 + a_j t + b_j \tag{3.59}$$

the *characteristic polynomial* of (3.55). The characteristic polynomial has the complex conjugate zeros $t_j^{(1,2)} = (B_j \pm i\,4/R)/A_j$. The zeros have the same moduli: $|t_j^{(1,2)}| = 1$, and therefore the classical *Theorem of Poincaré* (formulated below for the special case of a second–order difference equation) cannot be applied to distinguish two solutions with distinct asymptotic properties.

Theorem 3.9 (Poincaré Theorem, [14]). *Suppose that the zeros $t_j^{(1)}$, $t_j^{(2)}$ of the characteristic polynomial* (3.59) *have distinct moduli. Then for any nontrivial solution $s_j^{(n)}$ of* (3.55)

$$\lim_{n\to\infty} \frac{s_j^{(n+1)}}{s_j^{(n)}} = t_j^{(k)}$$

for $k = 1$ or $k = 2$.

REMARK 3.10. If equation (3.55) has characteristic roots with equal moduli then Poincaré's Theorem may fail (cf. example of Perron [14]).

It is well–known that the Legendre polynomials $P_n(\mu_j)$ and the *Legendre functions of the second kind* (of order zero) $Q_n(\mu_j)$ satisfy the same three–term recurrence relation (3.45). Therefore, the two linearly independent solutions to (3.55) are the convolution coefficients $s_{j,1}^{(n)} = s_j^{(n)}$ (3.48) and $s_{j,2}^{(n)}$ given by

$$s_{j,2}^{(n)} = \beta_j \frac{\lambda_j^{-n}}{2n-1}\big[Q_n(\mu_j) - Q_{n-2}(\mu_j)\big], \quad n \geq 2, \tag{3.60}$$

with some constant β_j.

Now we want to study the *asymptotic behaviour* of these two solutions. With the notation $\mu_j = \cos\theta_j$, $0 < \theta_j < \pi$, we use Lemma 3.6 which gives

$$P_n(\cos\theta_j) - P_{n-2}(\cos\theta_j) = -\frac{2\sqrt{2}\sqrt{\sin\theta_j}}{\sqrt{\pi}} \frac{\sin\big[(n-\frac{1}{2})\theta_j - \frac{\pi}{4}\big]}{\sqrt{n}} + \mathrm{O}(n^{-3/2}), \tag{3.61}$$

and from (3.48) we see that

$$s_j^{(n)} \sim -\alpha_j \frac{\sqrt{2}\sqrt{\sin\theta_j}}{\sqrt{\pi}} \lambda_j^{-n} \frac{\sin\big[(n-\frac{1}{2})\theta_j - \frac{\pi}{4}\big]}{(n-\frac{1}{2})\sqrt{n}}, \qquad n \to \infty. \tag{3.62}$$

An analogous formula to (3.33) for the Legendre functions of the second kind $Q_n(\mu_j)$ is given by the following Lemma:

LEMMA 3.11 (Theorem 8.21.14, [41]). *For* $0 < \theta_j < \pi$

$$Q_n(\cos\theta_j) = \frac{\sqrt{\pi}}{\sqrt{2}\sqrt{\sin\theta_j}} \frac{\cos\big[(n+\frac{1}{2})\theta_j + \frac{\pi}{4}\big]}{\sqrt{n}} + \mathrm{O}(n^{-3/2}). \tag{3.63}$$

This holds uniformly in the interval $[\varepsilon, \pi - \varepsilon]$.

As before we can deduce from (3.60) that

$$s_{j,2}^{(n)} \sim -\beta_j \frac{\sqrt{\pi}\sqrt{\sin\theta_j}}{\sqrt{2}} \lambda_j^{-n} \frac{\sin\big[(n-\frac{1}{2})\theta_j + \frac{\pi}{4}\big]}{(n-\frac{1}{2})\sqrt{n}}, \qquad n \to \infty \tag{3.64}$$

holds. Therefore the ratio of the two solutions behaves asymptotically as

$$\frac{s_{j,2}^{(n)}}{s_j^{(n)}} \sim \frac{\beta_j}{\alpha_j}\frac{\pi}{2}\frac{\sin\big[(n-\frac{1}{2})\theta_j + \frac{\pi}{4}\big]}{\sin\big[(n-\frac{1}{2})\theta_j - \frac{\pi}{4}\big]} = \frac{\beta_j}{\alpha_j}\frac{\pi}{2}\tan\big[(n-\frac{1}{2})\theta_j + \frac{\pi}{4}\big], \qquad n \to \infty,$$

i.e. neither $s_j^{(n)}$ nor $s_{j,2}^{(n)}$ can be a minimal solution. Consequently, the problem of determining the required values of the convolution coefficients is well–conditioned [16]: they can be computed numerically from the recurrence relation (3.49) in a stable fashion.

REMARK 3.12. In the special case $\theta_j = \pi/2$ we observe the asymptotic behaviour

$$\frac{s_{j,2}^{(n)}}{s_j^{(n+1)}} \sim \frac{\beta_j}{\alpha_j}\frac{\pi}{2}, \qquad n \to \infty.$$

Decay rate of the convolution kernel. Since $|\lambda_j| = 1$ the relation (3.62) shows that $s_0^{(n)}$, $s_j^{(n)} = \mathrm{O}(n^{-3/2})$, which agrees with the decay of the convolution kernel in the differential TBCs (2.8), (2.9). To show this property we consider the left TBC (2.9) and obtain after an integration by parts

$$\begin{aligned}\psi_x(0,t) &= c\,\frac{d}{dt}\int_0^t \frac{\psi(0,\tau)}{\sqrt{t-\tau}}\,d\tau \\ &= c\left[\frac{d}{dt}\int_{t-\varepsilon}^t \frac{\psi(0,\tau)}{\sqrt{t-\tau}}\,d\tau - \frac{1}{2}\int_0^{t-\varepsilon} \frac{\psi(0,\tau)}{(t-\tau)^{3/2}}\,d\tau + \frac{\psi(0,t-\varepsilon)}{\sqrt{\varepsilon}}\right]\end{aligned} \tag{3.65}$$

with

$$c = \sqrt{\frac{2}{\hbar\pi}}\,e^{-i\frac{\pi}{4}} = \frac{1-i}{\sqrt{\hbar\pi}}. \tag{3.66}$$

To compare the discrete convolution in the DTBCs with the continuous convolution in the differential TBCs we consider the following discretization (with $\varepsilon = \Delta t$)

$$-\frac{c}{2}\int_0^{t-\varepsilon} \frac{\psi(0,\tau)}{(t-\tau)^{3/2}}\,d\tau \approx -\frac{c}{2}\sum_{k=1}^{n-1} \psi_0^k\left[(n-k)\Delta t\right]^{-3/2}\Delta t. \tag{3.67}$$

If we compare this with (3.43a) written in the form

$$\frac{\psi_1^n - \psi_0^n}{\Delta x} = \frac{1}{\Delta x}\left[\sum_{k=1}^{n-1} s_0^{(n-k)}\psi_0^k - \psi_1^{n-1} + s_0^{(0)}\psi_0^n - \psi_0^n\right], \quad n \geq 1, \tag{3.68}$$

we would roughly expect

$$s_0^{(n)} \sim -\frac{c\Delta x}{2\sqrt{\Delta t}}\,n^{-3/2} = \frac{i-1}{2\sqrt{\hbar\pi}}\frac{\Delta x}{\sqrt{\Delta t}}\,n^{-3/2}, \quad n \to \infty. \tag{3.69}$$

In Figure 4 we compare the $s_0^{(n)}$ for increasing time levels n with the r.h.s. of (3.62). The used parameters are $\hbar = 1$, $\Delta t = 10^{-6}$, $\Delta x = 1/160$ and the potential is set to zero. Figure 4 displays a quite good agreement of the asymptotic behaviour of the $s_0^{(n)}$ with the predicted one in (3.62). The values of $s_0^{(n)}$ oscillate around the rate (3.69).

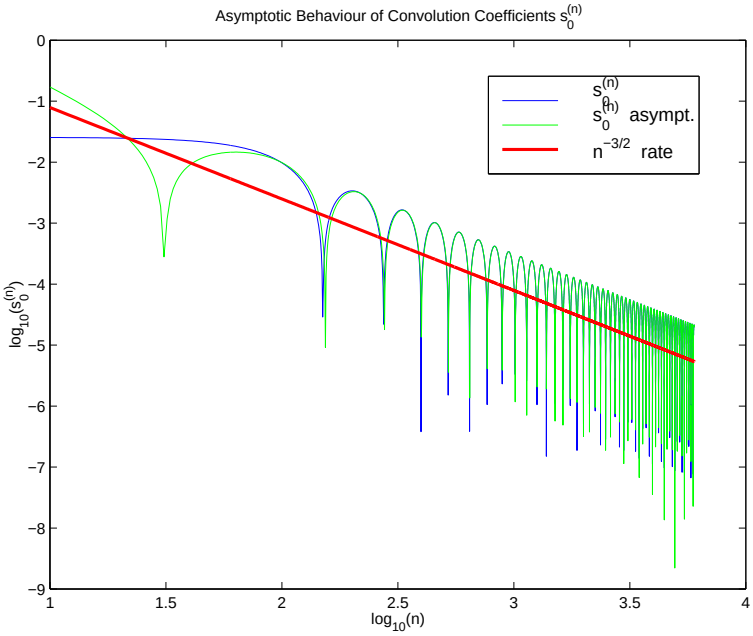

FIGURE 4. New discrete TBC: convolution coefficients $s_0^{(n)}$ compared to the r.h.s. of (3.62) and the decaying rate (3.69).

3.4. Stability of the resulting Scheme. We shall now discuss the stability of the Crank–Nicolson finite difference scheme in connection with the DTBCs (3.43).

Since the discrete whole–space solution satisfies the discrete TBCs (3.43), it is trivial that the implicit scheme (3.1), (3.43) for the IBVP can be solved at each time level n. To prove unique solvability and stability of the scheme, a discrete analogue of (2.19) can be derived. We sum up (3.2) for the finite interior range $j = 1, 2, \ldots, J-1$, use the *summation by parts* rule:

$$\Delta x \sum_{j=1}^{J-1} g_j D_x^- f_j = -\Delta x \sum_{j=0}^{J-1} f_j D_x^+ g_j + f_{J-1} g_J - f_0\, g_0 \tag{3.70}$$

and obtain (note that $D_x^2 = D_x^- D_x^+$)

$$\begin{aligned} \Delta x \sum_{j=1}^{J-1} \bar{\psi}_j^{n+\frac{1}{2}} D_t^+ \psi_j^n = &-\frac{i\hbar\Delta x}{2} \sum_{j=0}^{J-1} \left| D_x^+ \psi_j^{n+\frac{1}{2}} \right|^2 - \frac{i\Delta x}{\hbar} \sum_{j=1}^{J-1} V_j^{n+\frac{1}{2}} \left| \psi_j^{n+\frac{1}{2}} \right|^2 \\ &+ \frac{i\hbar}{2} \left[\bar{\psi}_J^{n+\frac{1}{2}} D_x^+ \psi_{J-1}^{n+\frac{1}{2}} - \bar{\psi}_0^{n+\frac{1}{2}} D_x^+ \psi_0^{n+\frac{1}{2}} \right]. \end{aligned} \tag{3.71}$$

Finally, taking the real part using (3.5) yields

$$D_t^+ \|\psi^n\|_2^2 = \hbar \Big[\mathrm{Re} \left\{ i\, \bar{\psi}_J^{n+\frac{1}{2}} D_x^- \psi_J^{n+\frac{1}{2}} \right\} - \mathrm{Re} \left\{ i\, \bar{\psi}_0^{n+\frac{1}{2}} D_x^+ \psi_0^{n+\frac{1}{2}} \right\} \Big], \tag{3.72}$$

with the discrete L^2–norm defined by $\|\psi^n\|_2^2 := \Delta x \sum_{j=1}^{J-1} |\psi_j^n|^2$. After summation with respect to the time index we get from (3.72):

(3.73)

$$\begin{aligned}\|\psi^{N+1}\|_2^2 &= \|\psi^0\|_2^2 + \hbar\Delta t\Big[\mathrm{Re}\,\{i\sum_{n=0}^{N} \bar\psi_J^{n+\frac12} D_x^- \psi_J^{n+\frac12}\} - \mathrm{Re}\,\{i\sum_{n=0}^{N} \bar\psi_0^{n+\frac12} D_x^+ \psi_0^{n+\frac12}\}\Big] \\ &= \|\psi^0\|_2^2 - \frac{\hbar\Delta t}{\Delta x}\,\mathrm{Re}\,\{i\sum_{n=0}^{N} \bar\psi_J^{n+\frac12}(\psi_J^{n+\frac12} * \tilde\ell_J^{(n)})\} - \frac{\hbar\Delta t}{\Delta x}\,\mathrm{Re}\,\{i\sum_{n=0}^{N} \bar\psi_0^{n+\frac12}(\psi_0^{n+\frac12} * \tilde\ell_0^{(n)})\},\end{aligned}$$

where $\tilde\ell_j^{(n)} := \ell_j^{(n)} - \delta_n^0$, $j = 0, J$. Again, as in the continuous case, it remains to show that the boundary–memory–terms in (3.73) are of *positive type*. We concentrate on the boundary term at $j = J$ and define the finite sequences

$$f_n = \psi_J^{n+\frac12} * \tilde\ell_J^{(n)}, \quad g_n = \psi_J^{n+\frac12}, \qquad n = 0, 1, \ldots, N, \tag{3.74}$$

with $f_n = g_n = 0$ for $n > N$, i.e. $\mathrm{Re}\,\{i\sum_{n=0}^{N} f_n\,\bar g_n\} \geq 0$ is to show. A $\mathcal{Z}$–transformation using the transformed DTBC (3.18) yields

$$\begin{aligned}\mathcal{Z}\{f_n\} = \hat f(z) &= \frac{z+1}{2}\,\hat\psi_J^N(z)\big[\nu_2(z) - 1\big] \\ &= \frac{iR}{4}\,\hat\psi_J^N(z)\Big\{\big[z - 1 + i\kappa(z+1)\big] \mp \sqrt[+]{Az^2 - 2Bz + C}\Big\},\end{aligned} \tag{3.75}$$

where $\hat\psi_J^N(z) = \sum_{n=0}^{N} \psi_J^n z^{-n}$ is analytic on $|z| > 0$. The expression above in the curly brackets is analytic for $|z| > 1$ and continuous for $|z| \geq 1$, since the zeros $z_{1,2}$ of the square root are given by $z_{1,2} = (B \pm i\,4/R)/A$ with $|z_{1,2}| = 1$. Therefore $\hat f(z)$ is analytic on $1 < |z| < \infty$. Note that we have to choose the sign in (3.75) such that it matches with $\nu_2(z)$ for $|z|$ sufficiently large. For the second sequence g_n we obtain

$$\mathcal{Z}\{g_n\} = \hat g(z) = \frac{z+1}{2}\,\hat\psi_J^N(z), \tag{3.76}$$

i.e. $\hat g(z)$ is analytic on $0 < |z| < \infty$.

Now the basic idea is to use *Plancherel's theorem* in the form

$$\sum_{n=0}^{\infty} f_n\,\bar g_n = \frac{1}{2\pi}\int_0^{2\pi} \hat f(e^{i\varphi})\,\overline{\hat g(e^{i\varphi})}\,d\varphi,$$

which gives

$$\begin{aligned}\mathrm{Re}\,\{i\sum_{n=0}^{N} f_n\,\bar g_n\} &= \frac{1}{8\pi}\,\mathrm{Re}\,\{i\int_0^{2\pi} |z+1|^2\,\big|\hat\psi_J^N(z)\big|^2\big[\nu_2(z) - 1\big]\Big|_{z=e^{i\varphi}} d\varphi\} \\ &= -\frac{1}{8\pi}\,\mathrm{Im}\,\{\int_0^{2\pi} \nu_2(e^{i\varphi})\,d\varphi\}.\end{aligned} \tag{3.77}$$

We remark that the pole of $\nu_2(z)$ at $z = -1$ is "cancelled" by $|z+1|^2$. From (3.77) we conclude that the discrete L^2–norm (3.73) is non–increasing in time if

$$\mathrm{Im}\;\nu_2(e^{i\varphi}) \leq 0, \qquad \forall\varphi \in [0, 2\pi], \tag{3.78}$$

holds. This property of ν_2 can be shown in the following way. If we define

$$y = -\frac{iR}{2}\Big(\frac{z-1}{z+1} + i\kappa\Big) \tag{3.79}$$

then (3.21) simply reads

$$\nu_2(y) = 1 + y - \sqrt[+]{y(2+y)}. \tag{3.80}$$

On the unit circle $z = e^{i\varphi}$, $0 \le \varphi \le 2\pi$, we have $(z-1)/(z+1) = i\tan(\varphi/2)$ and therefore

$$y = \frac{R}{2}\tan\frac{\varphi}{2} + \frac{R\kappa}{2} = \frac{(\Delta x)^2}{\hbar}\left[\frac{2}{\Delta t}\tan\frac{\varphi}{2} + \frac{V_L}{\hbar}\right], \qquad 0 \le \varphi \le 2\pi \tag{3.81}$$

is real. Consequently, $\nu_2(e^{i\varphi})$ becomes complex only in the interval $\varphi_a < \varphi < \varphi_b$, where φ_a, $\varphi_b \in [0, 2\pi]$ solve

$$\tan\frac{\varphi_a}{2} = -\Delta t\left(\frac{V_L}{2\hbar} + \frac{\hbar}{(\Delta x)^2}\right), \qquad \tan\frac{\varphi_b}{2} = -\frac{\Delta t}{2\hbar}V_L, \tag{3.82}$$

and we have the requested result

$$\text{Im } \nu_2(e^{i\varphi}) = -\text{ Im } \sqrt[+]{y(2+y)} \le 0, \qquad 0 \le \varphi \le 2\pi. \tag{3.83}$$

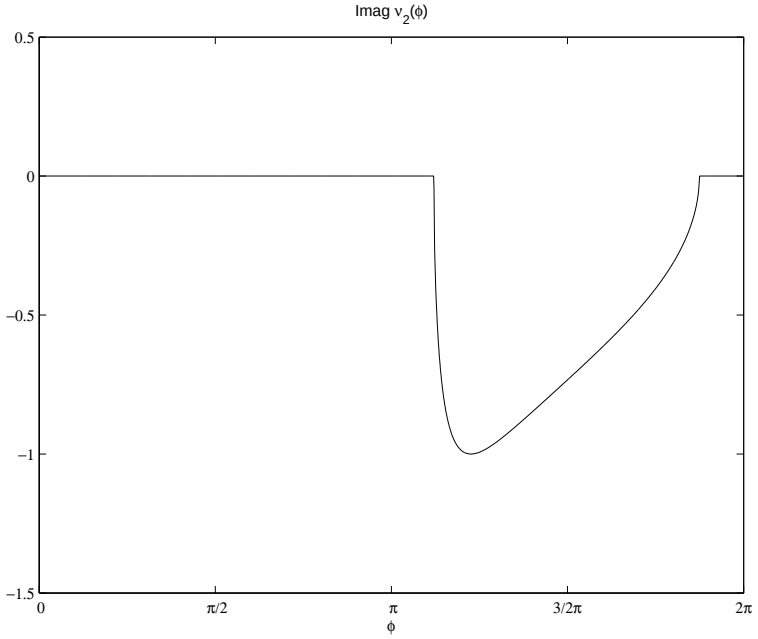

FIGURE 5. Imaginary part of $\nu_2(z)$ on the unit circle $z = e^{i\varphi}$, $0 \le \varphi \le 2\pi$.

The situation is illustrated in Figure 5, where we have set $\hbar = 1$, $V_L = 2 \cdot 10^4$ and used the parameters $\Delta x = 1/500$, $\Delta t = 2 \cdot 10^{-5}$. This gives the following values for φ_a, φ_b: $\varphi_a = 2\pi + 2\,\text{atan}(-5.2) \approx 3.5216$, $\varphi_b = 2\pi + 2\,\text{atan}(-0.2) \approx 5.8884$.

We then have the *main result* of this Section:

THEOREM 3.13 ([3]). *The solution of the discretized Schrödinger equation* (3.1) *with the discrete TBCs* (3.43) *is uniformly bounded*

$$\|\psi^n\|_2^2 := \Delta x \sum_{j=1}^{J-1} \left|\psi_j^n\right|^2 \leq \|\psi^0\|_2^2, \quad n \geq 1, \tag{3.84}$$

and the scheme is thus unconditionally stable.

REMARK 3.14. It can also be shown that (3.43) is a consistent discretization of the differential BCs (2.8), (2.9).

Simplified DTBC. The decay of the $s_j^{(n)}$ shown in (3.62) motivates to consider a *simplified version* of the DTBC (3.43) with the convolution coefficients cut off at an index M. This means that only the "recent past" (i.e. M time levels) is taken into account in the convolution in (3.43):

$$\psi_1^n - s_0^{(0)}\psi_0^n = \sum_{k=n-M}^{n-1} s_0^{(n-k)}\psi_0^k - \psi_1^{n-1}, \quad n \geq 1, \tag{3.85a}$$

$$\psi_{J-1}^n - s_J^{(0)}\psi_J^n = \sum_{k=n-M}^{n-1} s_J^{(n-k)}\psi_J^k - \psi_{J-1}^{n-1}, \quad n \geq 1. \tag{3.85b}$$

This, of course, reduces the perfect accuracy of the DTBC (3.43), but it is numerically cheaper while still yielding reasonable results for moderate values of M. We remark that the numerical stability of the scheme with simplified DTBC depending on the value of M is not anymore obtained automatically. This issue is currently under investigation [2].

3.5. Numerical Results. In this Section we present an example to compare the numerical results from using our new discrete TBC to the solution using other discretization strategies of the TBC for the Schrödinger equation (2.1). We also show the numerical effect if the DTBC is simplified by (3.85). Due to its construction, our DTBC yields exactly (up to round–off errors) the numerical whole–space solution restricted to the computational interval $[0, L]$. The calculation with discretized TBCs requires the same numerical effort. However, the solution may (on coarse grids) strongly deviate from the numerical whole–space solution.

Example. This example shows a simulation of a right travelling Gaussian beam $[\psi^I(x) = \exp(i100x - 30(x - 0.5)^2)]$ at four consecutive time steps evolving under the free Schrödinger equation ($\hbar = 1$) with the rather coarse space discretization $\Delta x = 1/160$ and the time step $\Delta t = 2 \cdot 10^{-5}$. Discretizing the analytic TBCs via (3.7) (scheme of Mayfield [30]) or as in Baskakov and Popov [6] induces strong numerical reflections. Our discrete TBCs (3.43), however, yield the smooth numerical solution to the whole–space problem, restricted to the computational interval $[0, 1]$ (up to round–off errors).

We observe in Figure 6 the artificial reflections travelling to the left induced by discretizing the analytic TBC while the solution with the new discrete TBC leave the computational domain without any numerical reflections. At time $t = 0.01$ the solution with the DTBC has almost completely left the domain $[0, 1]$ and the solutions with discretized TBCs contain a reflected wave packet with the maximum modulus (which corresponds to the maximum error) of around 0.17 for the approach of Mayfield and around 0.025 in case of the discretized TBC of Baskakov and Popov.

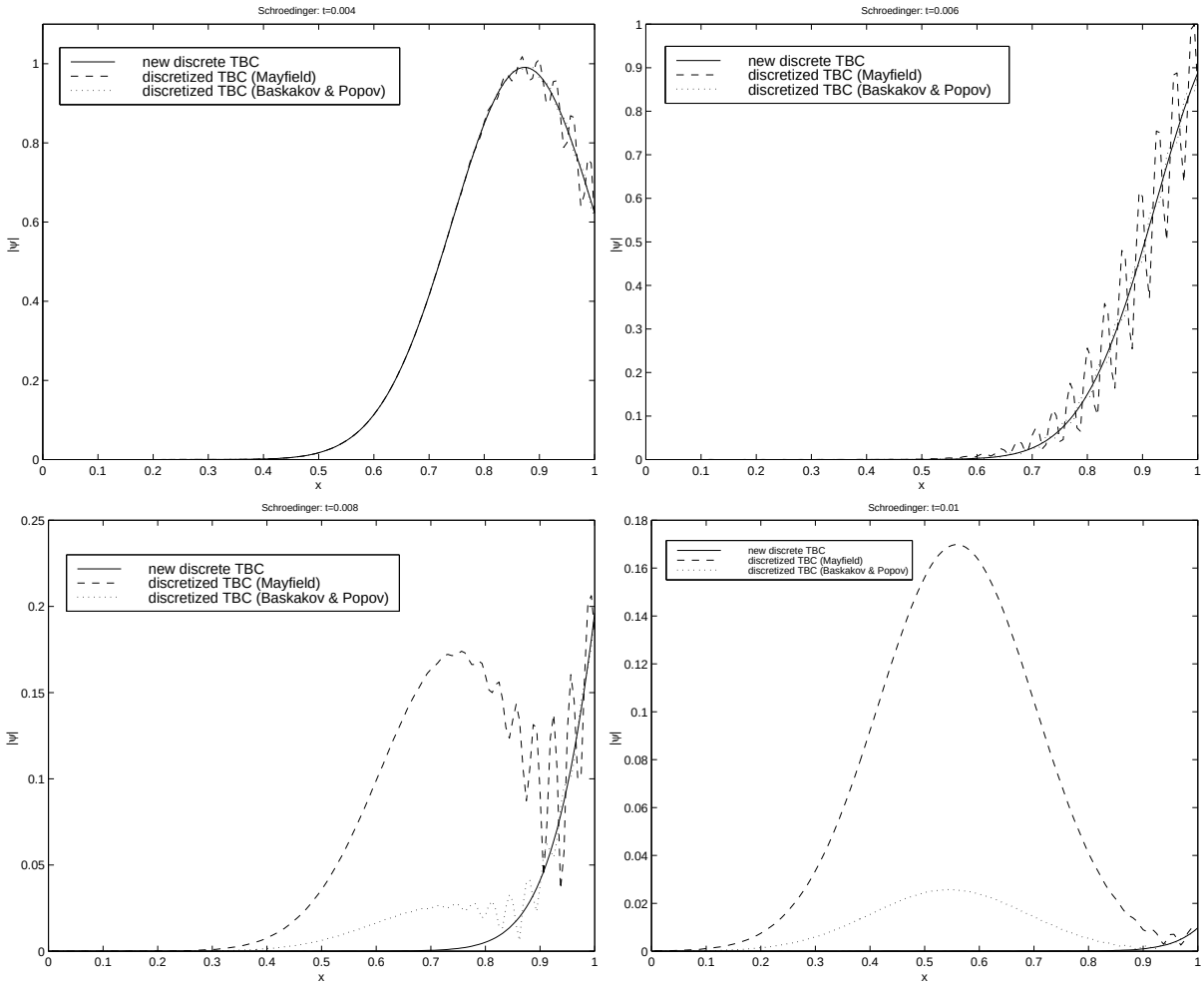

FIGURE 6. Solution $|\psi(x,t)|$ at time $t = 0.004$, $t = 0.006$, $t = 0.008$, $t = 0.01$: the solution with the new discrete TBCs (—) coincides with the whole–space solution, while the solution with the discretized analytic TBCs (3.7) from [30] (- - -) or from [6] ($\cdots$) introduces strong numerical reflections.

Now we present the results when using the simplified DTBC (3.85) and want to compare the outcome with the discretized TBCs at time $t = 0.01$. All these boundary conditions need a comparable computational effort. The *cut–off value* M is chosen appropriately, such that the simplified DTBC yields similar results with respect to the numerical reflections at the right boundary $x = 1$. As a reference we also plot the solution with the discrete TBCs ($\cdots$).

We see in Figure 7 that the solution with the simplified discrete TBCs (3.85) with $M = 5$ is already better than the solution with the discretized analytic TBCs (3.7) from [30].

We observe in Figure 8 that the error of the solution with the discretized analytic TBC from [6]. lies between the errors of the solutions with the simplified discrete TBCs (3.85) using the cut–off value $M = 30$, $M = 35$.

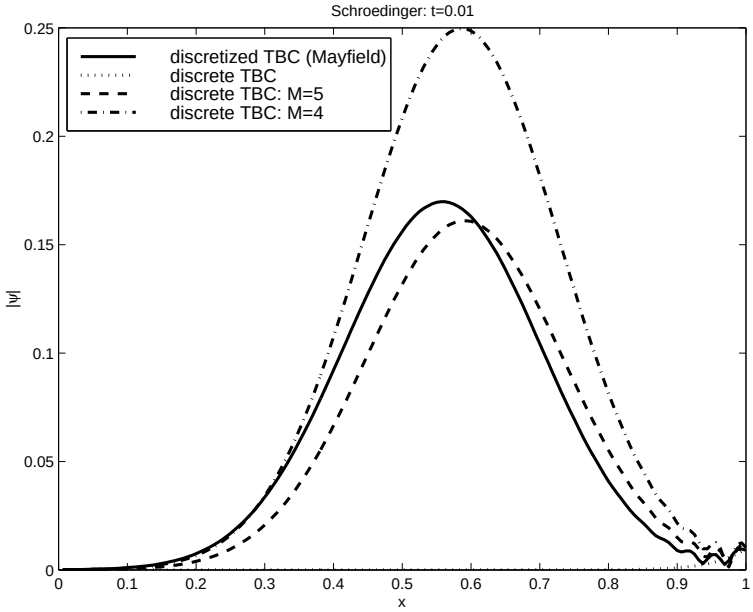

FIGURE 7. Solution $|\psi(x,t)|$ at time $t = 0.01$: the solution with the discretized TBCs of Mayfield [30] (—) in comparison to the solution using the simplified DTBC (3.85) with $M = 4$ (-.-.) and $M = 5$ (---).

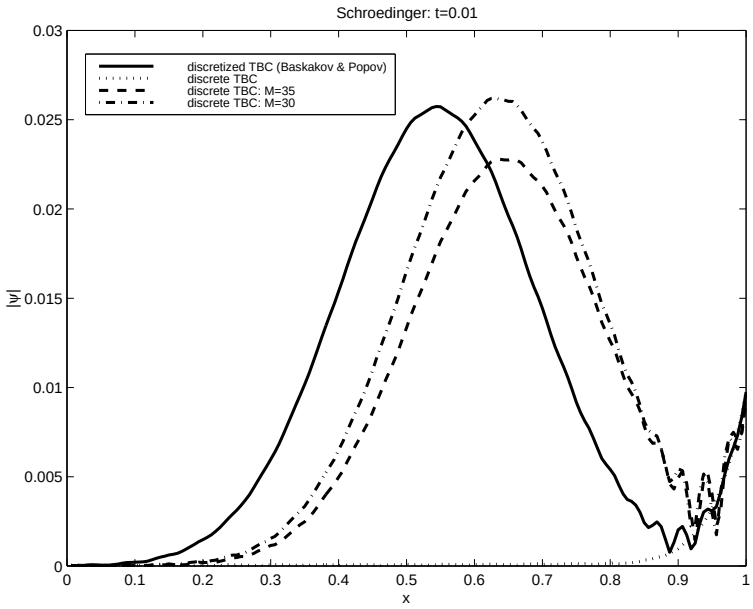

FIGURE 8. Solution $|\psi(x,t)|$ at time $t = 0.01$: the solution with the discretized TBCs of Baskakov and Popov [6] (—) in comparison to the solution using the simplified DTBC (3.85) with $M = 30$ (-.-.) and $M = 35$ (---).

4. DTBC for non–compactly supported Initial Data

In this Section we show how to drop assumption (A1), i.e. here the initial data $\psi^I(x)$ need not be compactly supported inside the computational domain. We only assume that

the initial function $\psi^I(x)$ is continuous. First we review the derivation of the TBC on the continuous level and mimick this derivation strategy afterwards for the discrete scheme.

4.1. The Transparent Boundary Condition. Here we review the derivation of the (continuous) TBC from [25]. In the case of the free Schrödinger equation with non–compactly supported initial data ψ^I the Laplace transformed right exterior problem (2.5) now reads

$$\hat{v}_{xx} + c^2 s\hat{v} = c^2\psi^I(x), \quad x > L, \tag{4.1a}$$

$$\hat{v}(L,s) = \hat{\Phi}(s), \tag{4.1b}$$

where we set $c = (1+i)/\sqrt{\hbar}$. Again, the idea is to solve this inhomogeneous second order differential equation (4.1) explicitly. The homogeneous solution is

$$\hat{v}_{hom}(x,s) = C_1(s)\, e^{ic\sqrt{s}(x-L)} + C_2(s)\, e^{-ic\sqrt{s}(x-L)}, \quad x > L, \tag{4.2}$$

and according to [22, (14.31)] a particular solution of (4.1a) is given by

$$\hat{v}_{par}(x,s) = \frac{c}{2i\sqrt{s}}\left[\int_L^x e^{ic\sqrt{s}(x-x')}\psi^I(x')\,dx' - \int_L^x e^{ic\sqrt{s}(x'-x)}\psi^I(x')\,dx'\right], \quad x > L, \tag{4.3}$$

i.e. the general solution is

$$\begin{aligned}\hat{v}(x,s) &= \hat{v}_{hom}(x,s) + \hat{v}_{par}(x,s)\\ &= \left[C_1(s)\, e^{-ic\sqrt{s}L} + \frac{c}{2i\sqrt{s}}\int_L^x e^{-ic\sqrt{s}x'}\psi^I(x')\,dx'\right] e^{ic\sqrt{s}x}\\ &+ \left[C_2(s)\, e^{ic\sqrt{s}L} - \frac{c}{2i\sqrt{s}}\int_L^\infty e^{ic\sqrt{s}x'}\psi^I(x')\,dx' + \frac{c}{2i\sqrt{s}}\int_x^\infty e^{ic\sqrt{s}x'}\psi^I(x')\,dx'\right] e^{-ic\sqrt{s}x}.\end{aligned} \tag{4.4}$$

We note that the last term in (4.4) is bounded for fixed s and $x \to \infty$. Since the solutions have to decrease as $x \to \infty$, the idea is to eliminate the growing factor $e^{-ic\sqrt{s}x} = e^{\frac{1-i}{\hbar}\sqrt{s}x}$ by simply choosing

$$C_2(s) = \frac{c}{2i\sqrt{s}}\int_L^\infty e^{ic\sqrt{s}(x'-L)}\psi^I(x')\,dx'. \tag{4.5}$$

Consequently, we obtain $C_1(s)$ from the boundary condition (4.1b):

$$C_1(s) = \hat{\Phi}(s) - \frac{c}{2i\sqrt{s}}\int_L^\infty e^{ic\sqrt{s}(x'-L)}\psi^I(x')\,dx'. \tag{4.6}$$

From this we get the following representation of the *transformed right TBC*:

$$\begin{aligned}\hat{v}_x(L,s) &= ic\sqrt{s}\, C_1(s) - \frac{c^2}{2}\int_L^\infty e^{ic\sqrt{s}(x'-L)}\psi^I(x')\,dx'\\ &= ic\sqrt{s}\,\hat{\Phi}(s) - c^2\int_L^\infty e^{ic\sqrt{s}(x'-L)}\psi^I(x')\,dx'.\end{aligned} \tag{4.7}$$

It remains to inverse transform (4.7). If we further assume that ψ^I is continuously differentiable, then integration by parts yields:

$$\hat{v}_x(L,s) = \frac{ic}{\sqrt{s}}\left[s\hat{\Phi}(s) - \psi^I(L)\right] - \frac{ic}{\sqrt{s}}\int_L^\infty e^{ic\sqrt{s}(x'-L)}\psi^I_x(x')\,dx'. \tag{4.8}$$

The inverse Laplace transformation using the convolution theorem gives

$$\psi_x(L,t) = \frac{ic}{\sqrt{\pi}} \int_0^t \frac{\psi_t(L,\tau)}{\sqrt{t-\tau}}\, d\tau - ic\, \mathcal{L}^{-1}\left\{ \frac{1}{\sqrt{s}} \int_L^\infty e^{ic\sqrt{s}(x'-L)} \psi_x^I(x')\, dx' \right\}. \tag{4.9}$$

Finally, if ψ_x^I is integrable for $x > L$, Levy proved ([25, Theorem 3.1]) that the integration and the inverse Laplace transform can be interchanged in (4.9) to obtain the *right TBC*

$$\psi_x(L,t) = \frac{ic}{\sqrt{\pi}} \int_0^t \frac{\psi_t(L,\tau)}{\sqrt{t-\tau}}\, d\tau - \frac{ic}{\sqrt{\pi t}} \int_L^\infty \psi_x^I(x)\, e^{\frac{i(x-L)^2}{2\hbar t}}\, dx. \tag{4.10}$$

REMARK 4.1. Clearly, if $\psi^I(x) = 0$ for $x > L$ then (4.10) reduces to the previously obtained right TBC (2.8) in the potential–free case (note that $-\sqrt{2}\, e^{-i\frac{\pi}{4}} = i - 1$).

As motivated in the previous Section we will not discretize this TBC. Instead we will show now how to derive the TBC on a fully discrete level by mimicking the derivation of the continuous TBC.

4.2. The Discrete Transparent Boundary Condition. First we show how to solve an inhomogeneous second order difference equation with constant coefficients of the form

$$U_{j+1} + a\, U_j + b\, U_{j-1} = \gamma_j\,, \qquad j \geq J-1. \tag{4.11}$$

We already know from Section 3 that the two linearly independent homogeneous solutions take the form α^j, β^j, $j \geq J$ with $\alpha\beta = b$. A particular solution V_j of (4.11) can be found with the ansatz of *"variation of constants"* [31], [14]:

$$V_{j-1} = c_j \alpha^{j-1} + d_j \beta^{j-1}, \quad j \geq J. \tag{4.12}$$

It follows that

$$V_j = c_{j+1}\alpha^j + d_{j+1}\beta^j = c_j\alpha^j + d_j\beta^j, \quad j \geq J-1, \tag{4.13}$$

if we force the condition

$$(\Delta^+ c_j)\, \alpha^j + (\Delta^+ d_j)\, \beta^j = 0 \tag{4.14}$$

to hold. Here Δ^+ denotes the usual forward difference operator, i.e. $\Delta^+ c_j = c_{j+1} - c_j$. Analogously, again assuming (4.14), we obtain for V_{j+1}

$$V_{j+1} = c_j \alpha^{j+1} + d_j \beta^{j+1} + (\Delta^+ c_j)\, \alpha^{j+1} + (\Delta^+ d_j)\, \beta^{j+1}. \tag{4.15}$$

Inserting (4.12), (4.13), (4.15) into the difference equation (4.11) gives

$$(\Delta^+ c_j)\, \alpha^{j+1} + (\Delta^+ d_j)\, \beta^{j+1} = \gamma_j\,, \tag{4.16}$$

together with the condition (4.14). This can easily be solved to obtain

$$\Delta^+ c_j = \frac{1}{\alpha - \beta}\, \alpha^{-j} \gamma_j\,, \quad \Delta^+ d_j = -\frac{1}{\alpha - \beta}\, \beta^{-j} \gamma_j\,, \tag{4.17}$$

i.e. we get the coefficients

$$c_j = c_J + \sum_{m=J}^{j-1} \Delta^+ c_m = c_J + \frac{1}{\alpha - \beta} \sum_{m=J}^{j-1} \alpha^{-m} \gamma_m, \quad j \geq J, \tag{4.18}$$

$$d_j = d_J + \sum_{m=J}^{j-1} \Delta^+ d_m = d_J - \frac{1}{\alpha-\beta} \sum_{m=J}^{j-1} \beta^{-m}\gamma_m, \quad j \geq J. \tag{4.19}$$

Consequently, the *particular solution* reads

$$\begin{aligned} V_j &= c_{j+1}\alpha^j + d_{j+1}\beta^j \\ &= \left[c_J + \frac{1}{\alpha-\beta}\sum_{m=J}^{j} \alpha^{-m}\gamma_m\right]\alpha^j + \left[d_J - \frac{1}{\alpha-\beta}\sum_{m=J}^{j}\beta^{-m}\gamma_m\right]\beta^j, \quad j \geq J-1, \end{aligned} \tag{4.20}$$

and the *general solution* of (4.11) is of the form

$$U_j = c\,\alpha^j + d\,\beta^j + \frac{1}{\alpha-\beta}\left[\sum_{m=J}^{j}\alpha^{j-m}\gamma_m - \sum_{m=J}^{j}\beta^{j-m}\gamma_m\right], \quad j \geq J-1, \tag{4.21}$$

which is the discrete analogue to the solution formula (4.3) in the continuous case.

Now we use (4.21) to design a boundary condition at $j = J$. For that purpose we assume $|\alpha| < 1$, $|\beta| > 1$ (recall that $b = \alpha\beta = 1$ for the Crank–Nicolson scheme for solving the Schrödinger equation). Proceeding analogously to the continuous case we have to eliminate the growing factor β^j by choosing d appropriately as

$$d = \frac{1}{\alpha-\beta}\sum_{m=J}^{\infty}\beta^{-m}\gamma_m. \tag{4.22}$$

We obtain from (4.21)

$$U_j = \left[c + \frac{1}{\alpha-\beta}\sum_{m=J}^{j}\alpha^{-m}\gamma_m\right]\alpha^j + \frac{1}{\alpha-\beta}\sum_{m=j+1}^{\infty}\beta^{j-m}\gamma_m, \quad j \geq J-1. \tag{4.23}$$

The value of c can be expressed with U_{J-1}:

$$c = \frac{U_{J-1}}{\alpha^{J-1}} - \left(\frac{\beta}{\alpha}\right)^{J-1}\frac{1}{\alpha-\beta}\sum_{m=J}^{\infty}\beta^{-m}\gamma_m, \tag{4.24}$$

and inserting this into (4.23) with $j = J$:

$$U_J = c\,\alpha^J + \frac{1}{\alpha-\beta}\sum_{m=J}^{\infty}\beta^{J-m}\gamma_m \tag{4.25}$$

yields

$$\begin{aligned} U_J &= \alpha\,U_{J-1} - \left(1-\frac{\alpha}{\beta}\right)\frac{1}{\alpha-\beta}\sum_{m=J}^{\infty}\beta^{J-m}\gamma_m \\ &= \alpha\,U_{J-1} - \beta^{-1}\sum_{m=0}^{\infty}\beta^{-m}\gamma_{J+m}, \end{aligned} \tag{4.26}$$

or equivalently

$$b\,U_{J-1} = \beta\,U_J + \sum_{m=0}^{\infty} b^{-m}\alpha^m\gamma_{J+m}. \tag{4.27}$$

Finally, we want to apply these results to the discretized Schrödinger equation (3.13) and derive the DTBC at $j = J$ in the situation, when the initial data ψ_j^0 does not vanish for $j \geq J-1$. In this case the *$\mathcal{Z}$–transformed right exterior Crank–Nicolson scheme reads*:

$$\hat{\psi}_{j+1}(z) - \left[2 - iR\Big(\frac{z-1}{z+1} + i\kappa\Big)\right] \hat{\psi}_j(z) + \hat{\psi}_{j-1}(z) = \frac{z}{z+1}\,\varphi_j\,, \quad j \geq J-1, \tag{4.28}$$

where the inhomogeneity φ_j is given by

$$\varphi_j = \Delta_x^2 \psi_j^0 + iR\psi_j^0 - R\kappa\psi_j^0, \quad j \geq J-1. \tag{4.29}$$

We can use (4.27) to obtain the *transformed right DTBC*:

$$\hat{\psi}_{J-1}(z) = \nu_2(z)\,\hat{\psi}_J(z) + \frac{z}{z+1} \sum_{m=0}^{\infty} \nu_1^m(z)\,\varphi_{J+m}, \tag{4.30}$$

where ν_1, ν_2 are the two solutions of the quadratic equation (3.17).

Remark 4.2. Again, (4.30) reduces to the DTBC (3.18) for $\varphi_j \equiv 0$.

In order to formulate the DTBC we define $(p_m^{(n)}) := \mathcal{Z}^{-1}\{\nu_1^m(z)\}$ and set $(\ell_J^{(n)}) := \mathcal{Z}^{-1}\{\nu_2(z)\}$. Using standard rules of inverse $\mathcal{Z}$–transforms (cf. [11], e.g.) we obtain by inverse transforming (4.30)

$$\psi_{J-1}^n - \ell_J^{(0)}\psi_J^n = \sum_{k=0}^{n-1} \ell_J^{(n-k)}\psi_J^k + (-1)^n\varphi_J + \sum_{m=1}^{\infty}\sum_{k=0}^{n} (-1)^{n-k} p_m^{(k)} \varphi_{J+m}, \quad n \geq 1. \tag{4.31}$$

Since the coefficients $\ell_J^{(n)}$ asymptotically alternate in time, this formulation can be improved and shortened by regarding once more $s_J^{(n)} := \ell_J^{(n)} + \ell_J^{(n-1)}$, which gives finally the *DTBC for non–compactly supported initial data*:

$$\psi_{J-1}^n - s_J^{(0)}\psi_J^n = \sum_{k=0}^{n-1} s_J^{(n-k)}\psi_J^k - \psi_J^{n-1} + \sum_{m=1}^{\infty} p_m^{(n)}\varphi_{J+m}, \quad n \geq 1. \tag{4.32}$$

Remark 4.3. Note that in contrast to the DTBC in Section 3 the r.h.s. (4.32) for $n = 1$ is not zero but

$$\psi_{J-1}^1 - \ell^{(0)}\psi_J^1 = s^{(1)}\psi_J^0 - \psi_J^0 + \sum_{m=1}^{\infty} p_m^{(1)}\varphi_{J+m}. \tag{4.33}$$

In practical situations the sum (over m) in (4.32) of course has to be finite (e.g. up to an index $m = M$). This means that the initial condition is still compactly supported, but possibly outside of the computational interval. The coefficients $p_m^{(n)}$, $m = 1, 2, \ldots, M$, can be calculated recursively by "continued convolution", i.e.

$$p_1^{(n)} = \mathcal{Z}^{-1}\{\nu_1(z)\}\,, \qquad p_2^{(n)} = \sum_{k=0}^{n} p_1^{(n-k)} p_1^{(k)}, \qquad p_3^{(n)} = \sum_{k=0}^{n} p_2^{(n-k)} p_1^{(k)}, \quad \text{etc..} \tag{4.34}$$

Since this computation is rather costly (even when using fast convolution algorithms with FFTs [32, Chapter 4]) we seek for another way to calculate

$$\tilde{S}_M^{(n)} := \sum_{m=1}^{M} p_m^{(n)}\varphi_{J+m}, \quad n \geq 1. \tag{4.35}$$

The key idea is to use the quadratic equation (3.17) for $\nu_1(z)$ in order to contruct a recurrence relation for the $p_m^{(n)}$ (w.r.t. m). Equation (3.17) for $\nu_1(z)$ gives

$$\begin{aligned}\nu_1^{m+1}(z) &= 2\left[1 - \frac{iR}{2}\Big(\frac{z-1}{z+1} + i\kappa\Big)\right]\nu_1^m(z) - \nu_1^{m-1}(z) \\ &= c_1\,\nu_1^m(z) - c_2\,\frac{z}{z+1}\,\nu_1^m(z) - \nu_1^{m-1}(z), \quad m \geq 1\end{aligned} \tag{4.36}$$

with $c_1 = 2 + iR + R\kappa$ and $c_2 = 2iR$. An inverse $\mathcal{Z}$–transformation gives

$$p_{m+1}^{(n)} = c_1 p_m^{(n)} - c_2 \sum_{k=0}^{n} (-1)^k p_m^{(n-k)} - p_{m-1}^{(n)}, \quad m \geq 1, \tag{4.37}$$

with the starting sequences $p_0^{(n)} = \delta_n^0$ and $p_1^{(n)} = \mathcal{Z}^{-1}\{\nu_1(z)\}$, $n \geq 0$. To circumvent the convolution in (4.37) we consider $q_m^{(n)} := p_m^{(n)} + p_m^{(n-1)}$, $p_m^{(-1)} = 0$ and obtain

$$q_{m+1}^{(n)} = c_1\, q_m^{(n)} - c_2\, p_m^{(n)} - q_{m-1}^{(n)}, \quad m \geq 1 \tag{4.38}$$

to use in the DTBC of the form

$$\psi_{J-1}^n - s_J^{(0)}\psi_J^n = \sum_{k=0}^{n-1} t_J^{(n-k)}\psi_J^k - \psi_J^{n-1} - \psi_{J-1}^{n-1} - \psi_J^{n-2} + \sum_{m=1}^{M} q_m^{(n)}\varphi_{J+m}, \quad n \geq 1, \tag{4.39}$$

where $t_J^{(n)} := s_J^{(n)} + s_J^{(n-1)}$. The calculations are done by the following algorithm

1. $q_0^{(n)} = \delta_n^0 + \delta_n^1 \quad n \geq 0$
2. $q_1^{(n)} = p_1^{(n)} + p_1^{(n-1)} = \tilde{s}_J^{(n)} \quad n \geq 0$
3. $S_1^{(n)} = q_0^{(n)}\varphi_J + q_1^{(n)}\varphi_{J+1} \quad n \geq 1$
4. `for` $m = 1, \ldots, M-1$ `do`

   $q_{m+1}^{(n)} = c_1\, q_m^{(n)} - c_2\, p_m^{(n)} - q_{m-1}^{(n)} \quad n \geq 0$

   $S_{m+1}^{(n)} = S_m^{(n)} + q_{m+1}^{(n)}\varphi_{J+m+1} \quad n \geq 1$

   $p_{m+1}^{(0)} = q_{m+1}^{(0)}$

   `for` $n = 1, \ldots, N$ `do`

   $p_{m+1}^{(n)} = q_{m+1}^{(n)} - p_{m+1}^{(n-1)}$

   `end`

`end`

Here N denotes the maximum time index. The computational effort of the above implementation of the DTBC is $\mathrm{O}(M \cdot N)$, and comparable to the effort when enlarging the computational domain sufficiently. The usage of the DTBC is especially beneficial when one needs several computations with the same exterior initial data. Then the calculation of the additional term has only to be done once. The same applies when the initial field is concentrated far outside the computational domain. This is the case in radiowave propagation when computing coverage diagrams of airborn antennas.

Alternatively, a second possible implementation is to consider the transformed DTBC (4.30) and to calculate numerically the inverse $\mathcal{Z}$–transform of the finite sum once:

$$F_n = \mathcal{Z}^{-1}\left\{ \frac{z}{z+1} \sum_{m=0}^{M} \nu_1^m(z)\, \varphi_{J+m} \right\}. \tag{4.40}$$

The DTBC then reads

$$\psi_{J-1}^n - \ell_J^{(0)} \psi_J^n = \sum_{k=0}^{n-1} \ell_J^{(n-k)} \psi_J^k + F_n, \quad n \geq 1. \tag{4.41}$$

The numerical inverse $\mathcal{Z}$–transformation will be the topic of the next section.

REMARK 4.4. While the DTBC (4.32) solves the problem of initial data that are supported outside of the computational domain, the resulting numerical effort of this approach is not completely settled yet and subject to further investigations. In particular one has to compare an "optimal" computation algorithm for the coefficients $p_n^{(m)}$or $q_n^{(m)}$ with simulations on a sufficiently enlarged computational domain.

4.3. Numerical Results. Here we present the numerical results when using our new discrete TBC (4.32) for the Schrödinger equation (2.1). We use the same initial data as in Section 3.5, but shifted such that it is partially outside the computational domain $0 \leq x \leq L$. Again, due to its construction, our DTBC yields exactly (up to round–off errors) the numerical whole–space solution restricted to the computational interval $[0, L]$.

Example. This example shows a simulation of a right travelling Gaussian beam $[\psi^I(x) = \exp(i100x - 30(x - 0.8)^2)]$ at three consecutive times evolving under the free Schrödinger equation ($\hbar = 1$) with the rather coarse discretization of 161 grid points for the interval $0 \leq x \leq 1$ (i.e. $\Delta x = 1/160$) and the time step $\Delta t = 2 \cdot 10^{-5}$. For the right exterior (computational) domain we choose the same space step Δx and use 60 grid points which results in the exterior interval $1 < x \leq 1.38125$.

In the following Figure 9 we plotted the absolute value of the initial data and the solution obtained with the discrete TBCs (4.32) at the time steps $t = 0.002$, $t = 0.004$, $t = 0.006$. One clearly sees in Figure 9 that the solution is solely propagated to the right and no artificial reflections are caused.

In this example the computation using the inhomogeneous DTBCs (4.32) needs approximately the same CPU–time than just enlarging the domain to the interval $0 \leq x \leq 1.8$ using a simple Neumann boundary condition at $x = 0$ and $x = 1.8$. From Figure 9 one can guess that the solution at $t = 0.004$ has already reached the right boundary at $x = 1.8$. Hence it is worthwhile in this example to use the inhomogeneous DTBCs whenever the solution for $t > 0.004$ is needed.

5. Numerical Inverse $\mathcal{Z}$–Transformations

The crucial point in the derivation of the DTBC in Section 3 was to find the exact inverse $\mathcal{Z}$–transformations. If it is not possible to calculate the convolution coefficients analytically then the inverse $\mathcal{Z}$–transformation can be performed numerically.

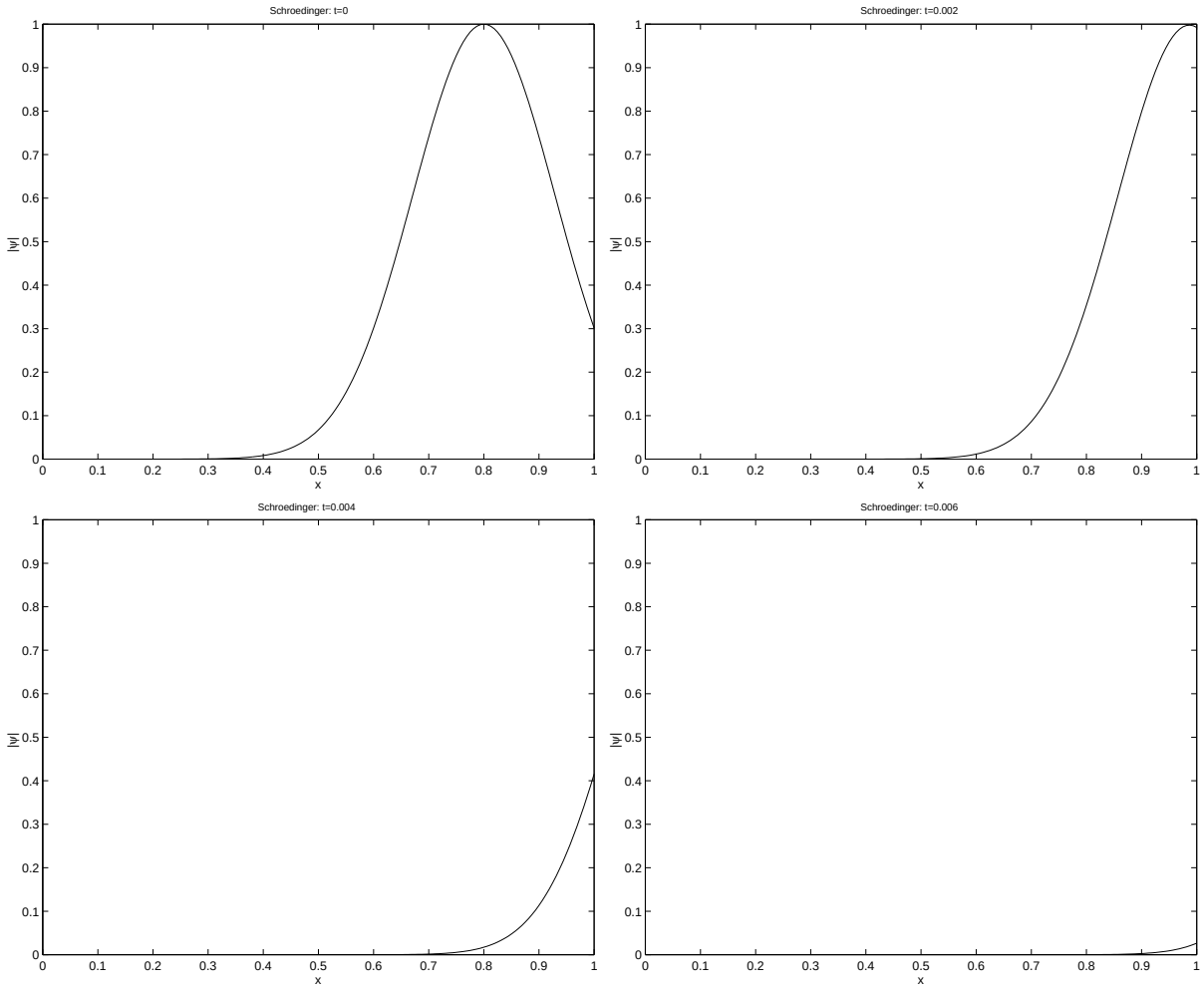

FIGURE 9. Solution $|\psi(x,t)|$ at time $t=0$, $t=0.002$, $t=0.004$, $t=0.006$: the solution with the new discrete TBCs (4.32) coincides with the whole–space solution and does not introduce any numerical reflections.

The numerical inversion of the $\mathcal{Z}$–transformation is based on the simple observation that the $\mathcal{Z}$–transformation of the sequence $\{f_n\}$, $n=0,1,\ldots$.

$$\mathcal{Z}\{f_n\} = \hat{f}(z) := \sum_{n=0}^{\infty} f_n\, z^{-n}, \quad z \in \mathbb{C}, \quad |z| > R^{-1}, \tag{5.1}$$

is nothing else but a Taylor series in $\tilde{z} = 1/z$, i.e. the problem of calculating the inverse $\mathcal{Z}$–transformation of $\hat{f}(z)$ is the numerical evaluation of the Taylor coefficients of the function $\tilde{f}(\tilde{z}) := \hat{f}(1/z)$. For that purpose we used here the FORTRAN subroutine ENTCAF (Evaluation of Normalized Taylor Coefficients of an Analytic Function) from Lyness and Sande [29].

First we want to outline the method. The *(normalized) Taylor coefficients* $r^n f_n$ can be obtained by *Cauchy's integral representation*:

$$r^n f_n = \frac{r^n}{2\pi i} \oint_{\mathcal{C}} \tilde{f}(\tilde{z})\, \tilde{z}^{-(n+1)} d\tilde{z}, \qquad r < R, \tag{5.2}$$

where $\mathcal{C}$ denotes a circle around the origin with radius r smaller than the radius of convergence R of the Taylor series. The approximation to f_n based on using an *N–point trapezoidal rule* for the contour integral is $f_n^{(N)}$ given by

$$r^n f_n^{(N)} = \frac{1}{N} \sum_{k=0}^{N-1} e^{-in\frac{2\pi k}{N}} f\big(re^{i\frac{2\pi k}{N}}\big), \qquad n = 0, 1, \ldots, N-1. \tag{5.3}$$

The approximation $r^n f_n^{(N)}$ is obtained by an iterative process. First approximations $f_0^{(N)}$, $N = 1, 2, 4, 8, \ldots$ are computed using (5.3). The convergence criterion is based on the knowledge of the exact value of the limit of the sequence: $\lim_{N\to\infty} f_0^{(N)} = f_0 = \tilde{f}(0)$. After converging the second part consists in evaluating (5.3) for $n = 0, 1, \ldots, N-1$ using the stored function values obtained in the first part. Since N is a power of 2 it is particularly appropriate to use a fast Fourier transform technique for this part.

The user has to specify the *required absolute accuracy* ε_{req} and the *radius of computation* r (the only restriction is that r must be less than R). ENTCAF returns an *accuracy estimate* ε_{est} together with approximations $r^n f_n^{(N)}$ and a number N, which are supposed to satisfy

$$\big|r^n f_n^{(N)} - r^n f_n\big| < \varepsilon_{est}, \qquad n = 0, 1, 2, \ldots, N-1, \tag{5.4a}$$

$$|r^n f_n| < \varepsilon_{est}, \qquad n = N, N+1, \ldots. \tag{5.4b}$$

We see from (5.4a) that this algorithm naturally delivers approximations $r^n f_n^{(N)}$ with a uniform bound on the discretization error. An output status parameter indicates to the user whether or not convergence or roundoff errors have occured. Exploiting the information of this output parameter one could construct a driver program which finds the appropriate value of r by itself.

Due to the asymptotic behaviour (3.36) it is not advisable to calculate the $\ell_j^{(n)}$. Instead we show how to compute the summed convolution coefficients $s_j^{(n)}$ numerically. The $s_j^{(n)}$ were defined by:

$$s_j^{(n)} := \ell_j^{(n)} + \ell_j^{(n-1)}, \quad n \geq 1, \quad s_j^{(0)} = \ell_j^{(0)}, \quad j = 0, J. \tag{5.5}$$

We concentrate on the right BC at $j = J$. If we assume $l_j^{(-1)} = 0$ we have:

$$\mathcal{Z}\{s_J^{(n)}\} = \nu_2(z) + z^{-1}\nu_2(z) = (1 + \tilde{z})\,\tilde{\nu}_2(\tilde{z}), \tag{5.6}$$

with $\tilde{\nu}_2(\tilde{z}) = \nu_2(z)$ and $\nu_2(z)$ given by formula (3.21).

5.1. Numerical Results. Here we present the numerical results when using the subroutine ENTCAF to compute the convolution coefficients $\ell_J^{(n)}$, $s_J^{(n)}$. In each example we chose $\varepsilon_{req} = 10^{-6}$ and set the *machine accuracy parameter* ε_M to 10^{-15}.

Example 1. The value for the potential V_L was set to $2 \cdot 10^4$ and the discretization parameter were taken from the example of Subsection 3.5, i.e. $\Delta x = 1/160$, $\Delta t = 2 \cdot 10^{-5}$. We used the computational radius $r = 0.92$. For that parameter choice ENTCAF returned a number of $N = 256$ nontrivial calculated coefficients and an estimated uniform absolute accuracy $\varepsilon_{est} = 9.8302 \cdot 10^{-7}$ in case of the coefficients $\ell_J^{(n)}$. For the summed coefficients $s_J^{(n)}$ we obtained $N = 128$ and $\varepsilon_{est} = 4.7684 \cdot 10^{-7}$. In the following Figure 10 we present the real and imaginary part of the numerically obtained coefficients in comparison to the exact values.

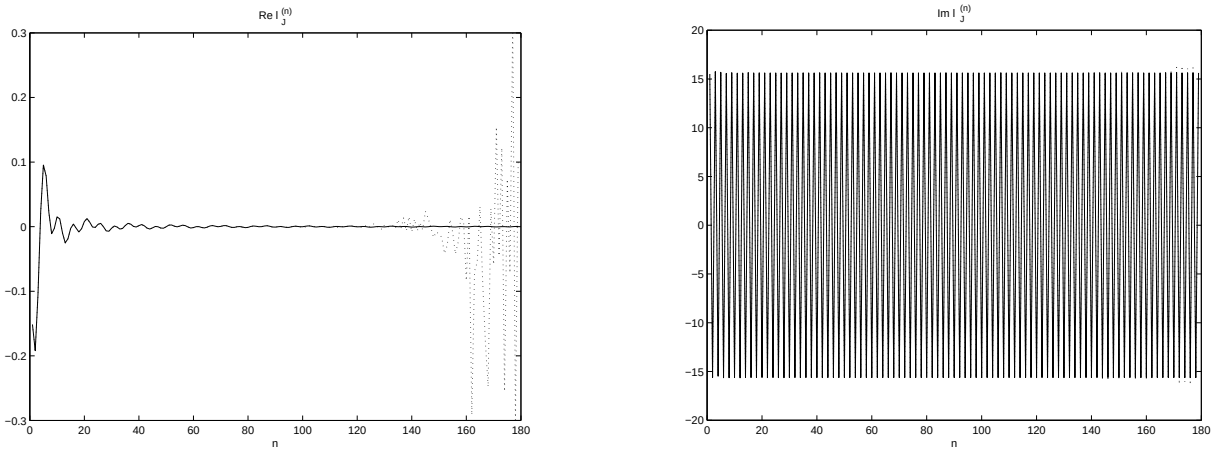

FIGURE 10. Example 1: Values for Re $\ell_J^{(n)}$, Im $\ell_J^{(n)}$

One serious problem is the *rescaling* of the computed coefficients. Since the algorithm yields approximations $r^n f_n^{(N)}$ with a uniform accuracy (5.4a) the computation is only reliable to a limited number of n when calculating $f_n^{(N)}$ from $r^n f_n^{(N)}$ for $r < 1$. Therefore some visible numerical errors occur in the calculation of Re $\ell_J^{(n)}$ for $n \geq 130$ and Im $\ell_J^{(n)}$ for $n \geq 170$.

On the left side of Figure 10 we observe the alternating behaviour shown in (3.36)

$$\ell_j^{(n)} \sim 2iR(-1)^n = i\,\frac{8}{\hbar}\frac{(\Delta x)^2}{\Delta t}(-1)^n = i\,\frac{125}{8}(-1)^n. \tag{5.7}$$

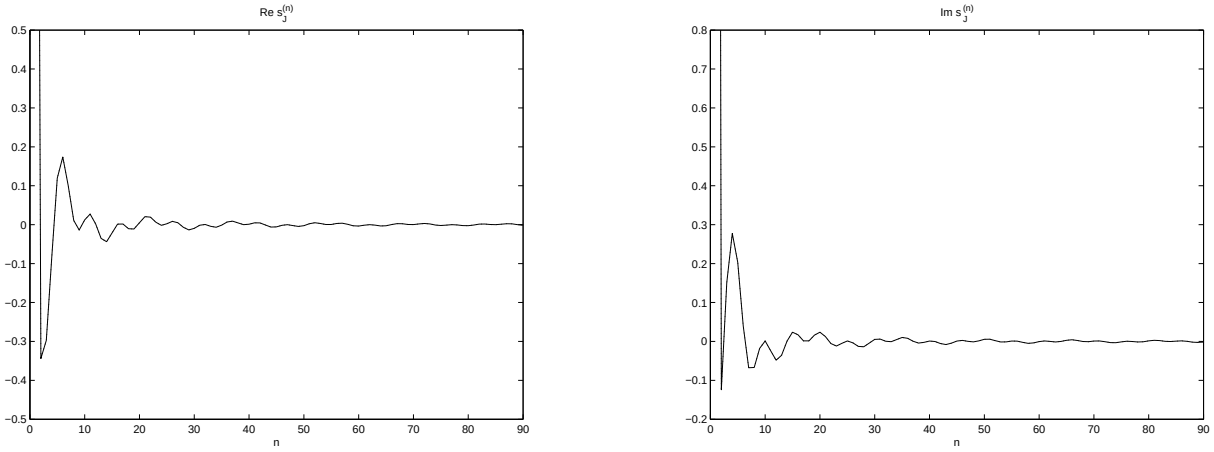

FIGURE 11. Example 1: Values for Re $s_J^{(n)}$, Im $s_J^{(n)}$.

Example 2. In this second example we set the potential to zero and changed the computational radius to $r = 0.95$ and the step sizes $\Delta x = 1/1600$, $\Delta t = 2 \cdot 10^{-4}$. For the coefficients $\ell_J^{(n)}$ ENTCAF returned a number of $N = 256$ nontrivial calculated coefficients and an estimated uniform absolute accuracy $\varepsilon_{est} = 2.9802 \cdot 10^{-6}$. In case of the summed coefficients $s_J^{(n)}$ we obtained $N = 128$ and $\varepsilon_{est} = 1.2288 \cdot 10^{-7}$. As before we show the real and imaginary part of the numerically obtained coefficients in comparison to the exact

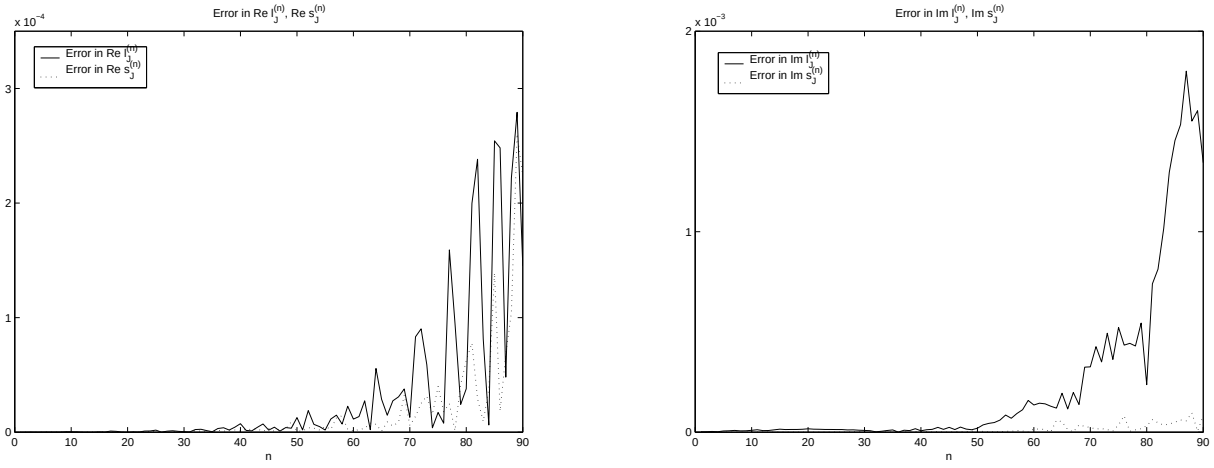

FIGURE 12. Example 1: Difference between the numerical and exact value of the real and imaginary part of $\ell_J^{(n)}$ (—) and $s_J^{(n)}$ $(\cdots)$.

values. Again, on the left side of Figure 13 one can see the alternating behaviour of the

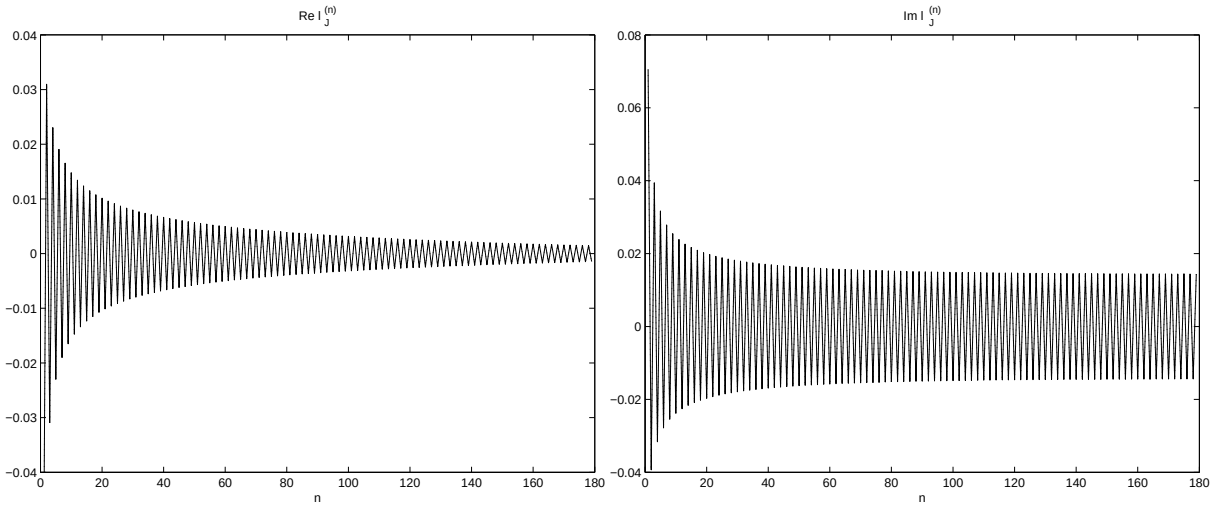

FIGURE 13. Example 2: Inverse $\mathcal{Z}$–transformation using ENTCAF: Numerically obtained values for Re $\ell_J^{(n)}$, Im $\ell_J^{(n)}$ compared to the exact ones.

coefficients $\ell_j^{(n)}$ and the numerical errors due to the rescaling of the computed coefficients for approximately $n \geq 30$.

Example 3. Finally we use the settings of the second example and intend to use a computational radius $r = 1$ to circumvent the problem of the rescaling. For the coefficients $\ell_J^{(n)}$ this cannot be done due to the singularity of $\nu_2(z)$ at $z = 1$. On the other hand, this singularity is removed in (5.6):

$$\begin{aligned} \mathcal{Z}\{s_J^{(n)}\} &= (1+\tilde{z})\,\tilde{\nu}_2(\tilde{z}) \\ &= 1 + \tilde{z} - \frac{iR}{2}\,y - \frac{iR}{2}\,\sqrt{\left(\frac{4i}{R}\,(1+\tilde{z}) + y\right)\,y}, \end{aligned} \tag{5.8}$$

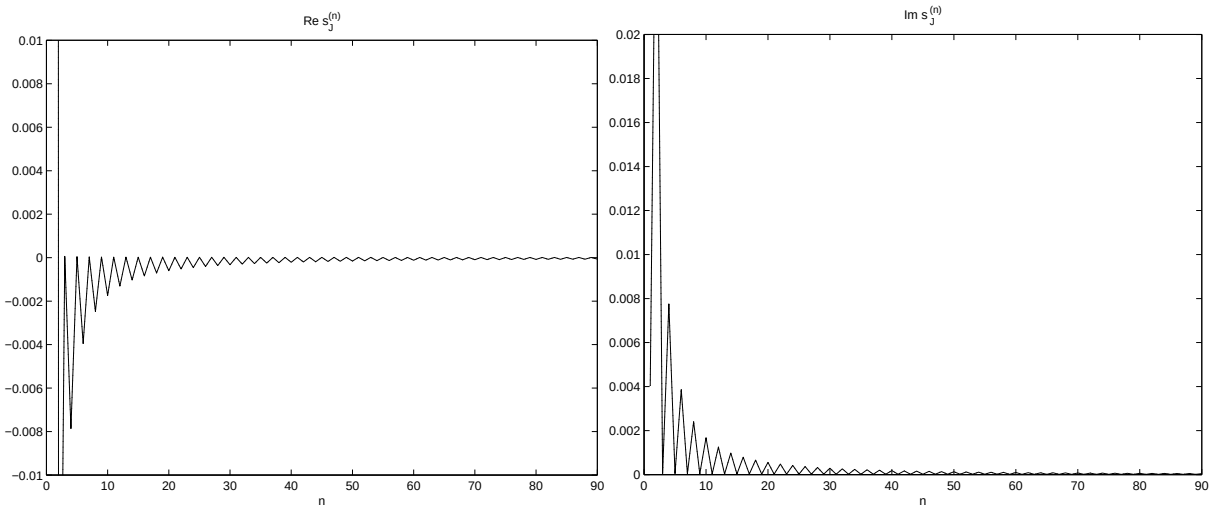

FIGURE 14. Example 2: Inverse $\mathcal{Z}$–transformation using ENTCAF: Numerically obtained values for Re $s_J^{(n)}$, Im $s_J^{(n)}$ compared to the exact ones.

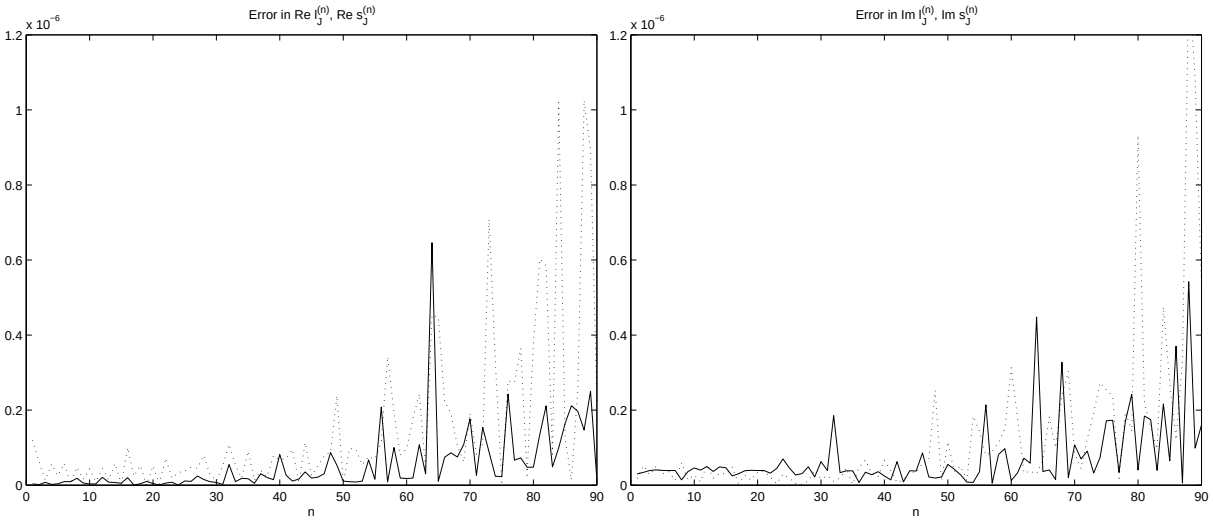

FIGURE 15. Example 2: Inverse $\mathcal{Z}$–transformation using ENTCAF: Difference between the numerical and exact value of the real and imaginary part of $\ell_J^{(n)}$ (—) and $s_J^{(n)}$ $(\cdots)$.

with the abbreviation $y = (1 - \tilde{z} + i\kappa(\tilde{z} + 1))$.

For the summed coefficients $s_J^{(n)}$ ENTCAF returned a number of $N = 1024$ nontrivial calculated coefficients and an estimated uniform absolute accuracy $\varepsilon_{est} = 2.2492 \cdot 10^{-6}$. The maximal absolute error for Re $s_J^{(n)}$ is $2.8609 \cdot 10^{-6}$ and $2.1455 \cdot 10^{-6}$ for calculating Im $s_J^{(n)}$.

Acknowledgement

Both authors were partially supported by the grants ERBFMRXCT970157 (TMR-Network) from the EU and the DFG under Grant-No. MA 1662/1-3. The second author acknowledges fruitful discussions with Prof. Weinan E.

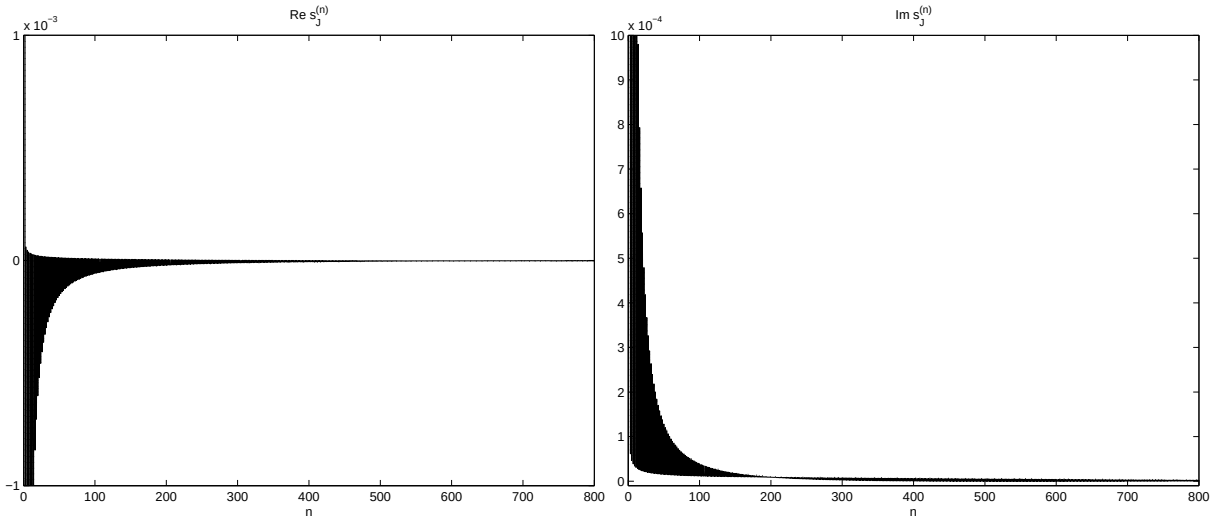

FIGURE 16. Example 3: Inverse $\mathcal{Z}$–transformation using ENTCAF: Numerically obtained values for Re $s_J^{(n)}$, Im $s_J^{(n)}$ compared to the exact ones. In both plots only one curve is visible since the results from both approaches match so closely.

Bibliography

[1] M. Abramowitz and I.A. Stegun, *Handbook of Mathematical Functions*, National Bureau of Standards, Applied Math. Series #55, Dover Publications, 1965.

[2] A. Arnold, M. Ehrhardt and I. Sofronov, work in progress.

[3] A. Arnold, *Numerically Absorbing Boundary Conditions for Quantum Evolution Equations*, VLSI Design **6** (1998), 313–319.

[4] A. Arnold, *Mathematical concepts of open quantum boundary conditions*, to appear in: Transp. Theory Stat. Phys., 2000.

[5] A. Bamberger, B. Engquist, L. Halpern and P. Joly, *Parabolic wave equation approximations in heterogeneous media*, SIAM J. Appl. Math. **48** (1988), 99–128.

[6] V.A. Baskakov and A.V. Popov, *Implementation of transparent boundaries for numerical solution of the Schrödinger equation*, Wave Motion **14** (1991), 123–128.

[7] E. Bécache, F. Collino, M. Kern and P. Joly, *Higher order numerical schemes for the paraxial wave equation*, Mathematical Methods in Geophysical Imaging III, 1995.

[8] J.F. Claerbout, *Coarse grid calculation of waves in inhomogeneous media with application to delineation of complicated seismic structure*, Geophysics **35** (1970), 407–418.

[9] J.F. Claerbout, *Fundamentals of Geophysical Data Processing*, McGraw–Hill, New York, 1976.

[10] L. Di Menza, *Approximations numériques d'équations de Schrödinger non linéaires et de modèles associés*, Ph.D. thesis, Université Bordeaux I, 1995.

[11] G. Doetsch, *Anleitung zum praktischen Gebrauch der Laplace-Transformation und der Z-Transformation*, R. Oldenburg Verlag München, Wien, 3. Auflage 1967.

[12] J. Douglas Jr., J.E. Santos, D. Sheen and L.S. Bennethum, *Frequency domain treatment of one–dimensional scalar waves*, Math. Mod. and Meth. in Appl. Sc. **3** (1993), 171–194.

[13] M. Ehrhardt, *Discrete Tranparent Boundary Conditions for Parabolic Equations*, Z. Angew. Math. Mech. **77** (1997) S2, 543–544.

[14] S.N. Elaydi, *An introduction to difference equations*, Undergraduate Texts in Mathematics, Springer, New York, 1996.

[15] B. Engquist and A. Majda, *Radiation Boundary Conditions for Acoustic and Elastic Wave Calculations*, Comm. Pure Appl. Math. **32** (1979), 313–357.

[16] W. Gautschi, *Computational aspects of three–term recurrence relations*, SIAM Rev. **9** (1967), 24–82.

[17] G. Gripenberg, S.-O. Londen and O. Staffans, *Volterra integral and functional equations*, Encyclopedia of Mathematics and Its Applications, 34. Cambridge Univ. Press, Cambridge, 1990.

[18] E. Hairer and G. Wanner, *Solving ordinary differential equations II: Stiff and differential-algebraic problems*, Springer Series in Computational Mathematics 14, 2nd rev. ed., Springer-Verlag (1996).

[19] L. Halpern, *Absorbing Boundary Conditions for the Discretization Schemes for the One–Dimensional Wave Equation*, Math. Comp. **38** (1982), 415–429.

[20] I. Harari, P.E. Barbone, M. Slavutin and R. Shalom, *Boundary infinite elements for the Helmholtz equation in exterior domains*, Int. J. Numer. Methods Eng. **41** (1998), 1105–1131.

[21] J.R. Hellums and W.R. Frensley, *Non–Markovian open–system boundary conditions for the time–dependent Schrödinger equation*, Phys. Rev. B **49** (1994), 2904–2906.

[22] H. Heuser, *Gewöhnliche Differentialgleichungen: Einführung in Lehre und Gebrauch*, Teubner, Stuttgart, 1989.

[23] P.K. Kythe, *An introduction to boundary element methods*, CRC Press, Boca Raton, FL.,1995.

[24] D. Lee and S.T. McDaniel, *Ocean acoustic propagation by finite difference methods*, Comput. Math. Appl. **14** (1987), 305–423.

[25] M.F. Levy, *Non–local boundary conditions for radiowave propagation*, in: Third International Conference on Mathematical and Numerical Aspects of Wave Propagation Phenomena, Juan-les-Pins, France, 24-28 April 1995.

[26] G. Lill, *Diskrete Randbedingungen an künstlichen Rändern*, Dissertation, Technische Hochschule Darmstadt, 1992.

[27] C. Lubich *Convolution Quadrature and Discretized Operational Calculus I*, Numer. Math. **52** (1988), 129–145.

[28] C. Lubich *On the multistep time discretization of linear initial–boundary value problems and their boundary integral equations*, Numer. Math. **67** (1994), 365–389.

[29] J.N. Lyness and G. Sande, *Algorithm 413: ENTCAF and ENTCRE: Evaluation of Normalized Taylor Coefficients of an Analytic Function*, Comm. ACM **14** (1971), 669–675.

[30] B. Mayfield, *Non–local boundary conditions for the Schrödinger equation*, Ph.D. thesis, University of Rhode Island, Providence, RI, 1989.

[31] R.E. Mickens, *Difference Equations: Theory and Applications*, 2nd ed., Van Nostrand Reinhold, New York, 1990.

[32] H.J. Nussbaumer, *Fast Fourier transform and convolution algorithms*, Springer Series in Information Sciences Vol. 2. Springer–Verlag, 1981.

[33] J.S. Papadakis, *Impedance formulation of the bottom boundary condition for the parabolic equation model in underwater acoustics*, NORDA Parabolic Equation Workshop, NORDA Tech. Note 143, 1982.

[34] J.S. Papadakis, M.I. Taroudakis, P.J. Papadakis and B. Mayfield, *A new method for a realistic treatment of the sea bottom in the parabolic approximation*, J. Acoust. Soc. Am. **92** (1992), 2030–2038.

[35] J.S. Papadakis, *Impedance Bottom Boundary Conditions for the Parabolic–Type Approximations in Underwater Acoustics*, in: Advances in Computer Methods for Partial Differential Equations VII, eds. R. Vichnevetsky, D. Knight, and G. Richter, IMACS, New Brunswick, NJ, 1992, pp. 585–590.

[36] C.W. Rowley and T. Colonius, *Discretely Nonreflecting Boundary Conditions for Linear Hyperbolic Systems*, J. Comp. Phys. **157** (2000), 500–538.

[37] A. Schädle, *Numerische Behandlung transparenter Randbedingungen für die Schrödinger–Gleichung*, Masters Thesis, Universität Tübingen, 1998.

[38] F. Schmidt and P. Deuflhard, *Discrete transparent boundary conditions for the numerical solution of Fresnel's equation*, Comput. Math. Appl. **29** (1995), 53–76.

[39] F. Schmidt and D. Yevick, *Discrete transparent boundary conditions for Schrödinger–type equations*, J. Comp. Phys. **134** (1997), 96–107.

[40] J.C. Strikwerda, *Finite Difference Schemes and Partial Differential Equations*, Wadsworth & Brooks/Cole, 1989.

[41] G. Szegö, *Orthogonal Polynomials*, Amer. Math. Soc. Colloquium Publications 23, 3rd ed. 1967.

[42] D.J. Thomson and M.E. Mayfield, *An exact Radiation Condition for Use with the A Posteriori PE Method*, J. Comp. Acous. **2** (1994), 113–132.

[43] L. Wagatha, *On Boundary Conditions for the Numerical Simulation of Wave Propagation*, Appl. Num. Math. **1** (1985), 309–314.

[44] J.C. Wilson, *Derivation of boundary conditions for the artificial boundaries associated with the solution of certain time dependent problems by Lax–Wendroff type difference schemes*, Proc. Edinb. Math. Soc. **II. Ser. 25** (1982), 1–18.